Design of a battery balancing prototype

Gernot Hehn

Graz May 23, 2010

EIDESSTATTLICHE ERKLÄRUNG

Ich erkläre an Eides statt, dass ich die vorliegende Arbeit selbstständig verfasst, andere als die angegebenen Quellen/Hilfsmittel nicht benutzt und die den benutzten Quellen wörtlich und inhaltlich entnommenen Stellen als solche kenntlich gemacht habe.

Graz, am May 23, 2010 .....
(Unterschrift)

Englische Fassung:

STATUTORY DECLARATION

I declare that I have authored this thesis independently, that I have not used other than the declared sources / resources and that I have explicitly marked all material which has been quoted either literally or by content from the used sources.

May 23, 2010 .....
(signature)

1 Acknowledgements

I want to thank

- austriamicrosystems
- Ass. Prof. Dr. Di. Gunter Winkler for many hours of discussion, helpful advice and good guidance throughout the creation of this thesis
- Di. Manfred Brandl for getting me started on my project at austrimicrosystems and giving me insight in semiconductor design proecesses.
- My collegues at austriamicrosystems for their helpful suggestion and for their friendly attitude.

2 Abstract

Managing batteries in a lot of different applications has become vital for mobile devices from things as omnipresent as a cell-phone to battery powered cars. The challenge of keeping batteries within their specified operating parameters has been targeted with a lot of specialised hardware. This work concentrates on battery balancing (the part of battery management that keeps batteries at an equal charge state throughout a battery stack). It provides a prototype for an IC implementation of a self contained battery balancing system that is scalable from a few cells (used e.g. in electric power tools) up to hundreds of cells (for electric cars) and uses active charge redistribution in contrast to wasting excessive energy in heat. The advantage of not having to design a specialized hardware for each individual application as well as the higher efficiency make it a recognizable alternative to traditional approaches.

Contents

3 Lithium Batteries

3.1 Basics

One of the important things to understand about lithium batteries is that the term 'Lithium Battery' subsumes a whole lot of different battery chemistries presently in use. In fact the technology in this field is still changing, so even an outline of existing technologies would be incomplete. However there are a few topologies that are widely used and they do have a lot in common. So I will describe the chemical process that basically drives all these batteries and then explain the differences between the various types and resulting effects on battery handling.

A Lithium Battery's main components are:

1. The negative electrode (anode) For the moment graphite carbon is the most commonly used for its good surface area versus weight ratio as well as its easy manufacturability. There are types which use a nano structured lithium titanat electrode [2] or pure lithium [3] to increase capacity dramatically, but they are still under development.

Anode Material	Average Voltage	Gravimetric Capacity	Gravimetric Energy
Graphite (LiC6)	0.1-0.2 V	372 mAh/g	0.0372-0.0744 kWh/kg
Titanate (Li4Ti5O12)	1-2 V	160 mAh/g	0.16-0.32 kWh/kg
Si (Li4-4Si)	0.5-1 V	4212 mAh/g	2.106-4.212 kWh/kg
Ge (Li4-4Ge)	0.7-1.2 V	1624 mAh/g	1.137-1.949 kWh/kg

Table 3.1: Comparison of different Anode materials [1]

2. The positive electrode (cathode) Its composition is very individual for each cell and is typically used to distinguish the different battery chemistries.
   We distinguish between:

Cathode Material	Average Voltage	Gravimetric Capacity	Gravimetric Energy
LiCoO2	3.7 V	140 mAh/g	0.518 kWh/kg
LiMn2O4	4.0 V	100 mAh/g	0.400 kWh/kg
LiNiO2	3.5 V	180 mAh/g	? kWh/kg
LiFePO4	3.3 V	150 mAh/g	0.495 kWh/kg
Li2FePO4F	3.6 V	115 mAh/g	0.414 kWh/kg
LiCo1/3Ni1/3Mn1/3O2	3.6 V	160 mAh/g	0.576 kWh/kg
Li(NixMnyCoz)O2	4.2 V	220 mAh/g	0.920 kWh/kg

Table 3.2: Comparison of different Cathode materials [1]

   Among cathode materials the most commonly used is LiCoO2 for its high energy density although LiMn2O4 is also frequently used for its higher discharge rating and Li2FePO4F (or short lithium iron phosphate) batteries are becoming more and more recognized for their robustness (which is essential for automotive applications).

3. A seperator isolating anode and cathode.
   Research has shown that by making the separator more rugged (e.g. using a ceramic separator) the overall robustness of a Li-Battery can be significantly increased.

4. The electrolyte.
   We differentiate between:
   - Liquid electrolytes like LiPF6, LiBF4 or LiClO4 in an organic water free solvent
   - Polymers and polyvinyl-fluoride (hence the name Lithium-Polymer Battery)
   - Lithium-iron-phosphate Li3P04N

   Generally liquid electrolytes are used for high capacity applications and polymerised electrolytes for high energy application. So let us take a look at the most commonly used type which is a cobalt cathode, graphite anode liquid electrolyte.

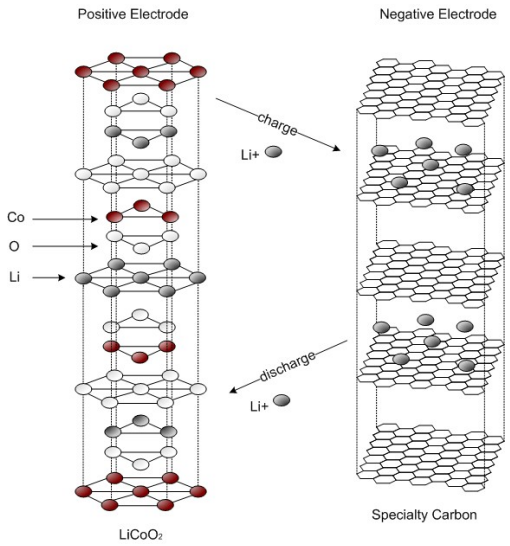

Figure 3.1: Chemical reaction of a Li-Battery [4]

The chemical reaction that allows the battery to function is as follows:

$$LiCoO_2 + C_6 \underset{\text{discharge}}{\overset{\text{charge}}{\rightleftharpoons}} Li_{1-x}CoO_2 + C_6L_x \quad [4]$$

Lithium in the positive electrode material is ionized during charge and moves from layer to layer in the negative electrode (as shown in the left image). During discharge Li ions move to the positive electrode where it embodies the original compound.
The overall reaction is limited. Overdischarge will supersaturate lithium cobalt oxide, leading to the production of lithium oxide, which is an irreversible reaction
Figure 3.1 shows the chemical interaction of a Li-Battery.

3.2 Distinctions to traditional battery chemistries

The most commonly used battery chemistries before the introduction of lithium technology were Ni-Cd and Ni-Mh. As there are some significant differences between these types of batteries and Lithium powered batteries, let me point out the important ones:
Advantages:

- The average capacity per gram is double to triple the one of classic batteries. This makes it possible to power modern mobile devices that have an ever higher energy consumption due to added features. It also allows reducing battery size and as such the size of devices that use them.

- The voltage per cell is between 3,3 to 3,8 V/cell which is roughly three times that of a classic cell. This enables operating devices from a single cell which means robuster construction and fewer errors because of missing interconnections.
- The voltage is very constant throughout the whole discharging cycle. It only drops significantly at the very end of the battery's capacity reserves. This makes it easy to design electronics that can use the whole of the battery's charge but also makes it a lot more difficult to diagnose the battery's state of charge correctly.
- The layers of anode cathode and separator are very thin, which permits construction of Li-Batteries in a wide variety of shapes so they will fit into pretty much any space.
- Li-Batteries do not suffer from effects like the Memory-Effect. They do also have a way lower self discharge rate of approximately 5% per month compared to over 30% for conventional batteries.

Disadvantages:

- One significant disadvantage is the Li-Batteries' poor cycle life. They do lose capacity with every charge and the internal resistance increases diminishing their ability to drive high currents.
- High charge states over a prolonged time as well as higher temperatures (above 40°C) also have a negative influence on both capacity and internal resistance.
- Li-Batteries must never be overcharged, discharged under a certain level or charged/discharged with too high a current. This leads to internal damage and may result in rupturing of the separator and finally destruction of the battery (possibly causing the battery to catch fire).
- Therefore Li-Batteries need additional safety electronics, which will be dicussed later.

3.3 Comparison of performance data

Chemistry:	NiCd	NiMH	Lead Acid	Li-ion	Li-polymer
Gravimetric Energy Density (Wh/kg)	45-80	60-120	30-50	150-220	130-280
Volumetric Energy Density (Wh/l)	150-250	250-400	50-100	250-530	300-600
Power Density (W/kg)				300-1500	300-2800
Internal Resistance (mOhm)	100 to 200	200 to 300	$\leq$ 100	150 to 250	200 to 300
Cycle Life (to 80% of initial capacity)	1500	300 to 500	200 to 300	500 to 1000	300 to 500
Fast Charge Time	1h typical	2-4h	8-16h	1-4h	0.5-1h
Overcharge Tolerance	moderate	low	high	very low	very low
Cell Voltage (nominal)	1.25V	1.25V	2V	3.6V	3.7V
Load Current:					
- peak	20C	5C	5C	$\geq$ 2C	$\geq$30C
- best result	1C	0.5C or lower	0.2C	1C or lower	1C - 5C
Operating Temperature	-40 to 60°C	-20 to 60°C	-20 to 60°C	-20 to 60°C	0 to 60°C
Commercial use since	1950	1990	1970	1991	1999

Table 3.3: Performance Figures for different Battery Chemistries

As can be seen in the table 3.3 and the figure 3.2 above li-battery technology has huge advantages against the older batter technologies. Therefore it provides a bunch of new opportunities for mobile applications. But there still is a huge gap if we are to compare the energy density of known battery chemistries against that of carbon fuel (compare table 3.4).

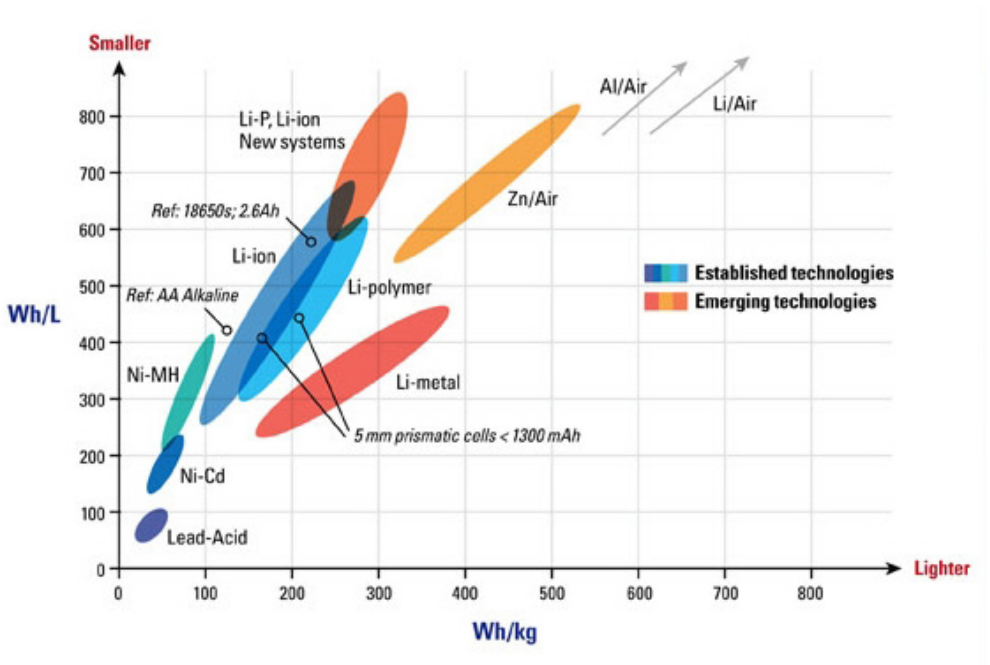

Figure 3.2: Energy Density Comparison [9]

	Gasoline	Diesel	Hydrogen
Gravimetric Energy Density (Wh/kg)	12200	13800	33300
Volumetric Energy Density (Wh/l)	9700	10942	530

Table 3.4: Performance Figures for fossile energy

3.4 Treatment of Li-Cells

Charging:
The most commonly used technique to charge Li-Cells is the so called CC/CV method which is short for constant current / constant voltage. Basically the cells are charged with their nominal charging current (typically 1C, which means once their capacity, so for a 2AH battery that would be 2A) until their cell voltage has reached the typical cell end voltage of the battery chemistry in use (typically between 4 and 4,2 V). After that the voltage is held at a constant level while the current decreases until it drops below approximately 5% of the nominal charging current, at which point the battery is considered fully charged. The constant voltage part is the critical part in charging these batteries. It is necessary to keep this voltage at least within a 50mV range of

the desired voltage otherwise the battery will take damage.

Discharging:
Discharging conditions vary a lot depending on the device(s) the battery is powering. But there are a few conditions that must never be neglected.

- The discharge current has to stay safely below the maximum rated current.
- The battery (and any of its cells) must never be discharged below a certain voltage (and therefore capacity).
- The temperature of each individual cell has to stay within a certain safe operating range (which is typically $0-40°C$ although there are types that can handle more temperature stress)
- Short circuit and reverse polarity have to be prevented at all times

The above described aspects call for a circuitry that monitors all the battery's health parameters and prevents damage of the battery. The circuit's essential functions are the following:

- Check charge and discharge current and disconnect battery if the current reaches the specified limits.
- Regulate temperature of battery either through active cooling/heating or through decrease of the load/charge current
- Check voltages of individual cells and equalize the charge over all cells (this process is called balancing)

To meet the requirements the battery monitoring system has to know the three main parameters of a battery which are:

- SOC ... State Of Charge
  State of charge describes the actual capacity of the whole battery at the moment. As the state of charge can't be measured directly two indirect methods are mostly used in combination.
  - Method 1: Voltage over Capacity Diagram The cell voltage changes with its remaining capacity. As one can see in figure 3.3 the curves are not only pretty flat (meaning the voltage change is minimal in comparison to the capacity change) but also change with the discharge current. And as if that wasn't enough there is also hysteresis. Meaning that the voltage increases only slowly to its nominal value after a zero load condition and vice versa after charging.
  - Method 2: Coulomb Counting: With this method the battery monitor calculates the power that is flowing in or out of the battery and multiplies it with time, giving the total energy remaining in the battery. If the charge

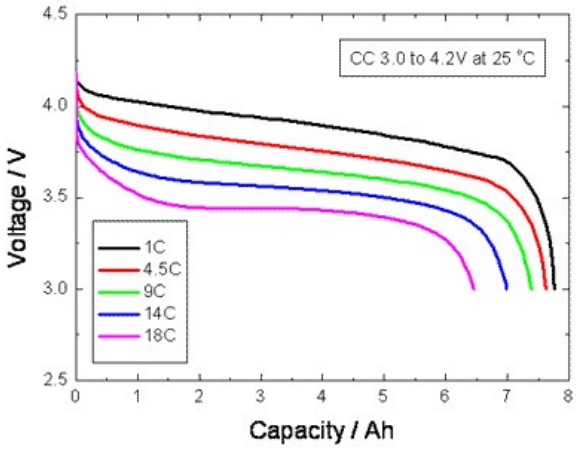

Figure 3.3: Lithium Battery Discharge curves

state is known at the beginning of the measurement this method can give you a good estimate of the actual charge even under load.

As mentioned before in reality those two methods are often combined (mostly using a kalman filter or fuzzy logic implementation) to give more reliable information on the actual state of charge.

- SOH ... State Of Health
  'The State of Health reflects the general condition of a battery compared to a new battery. It is a measure for the aging process that takes place in every battery, taking into account such factors as charge acceptance, internal resistance, voltage and self-discharge.' [9] There is no way to measure state of health directly. The function is mostly implemented through a logbook function which compares the parameters of the last few charge and discharge cycles against a lookup table with battery conditions throughout a lifecycle or with the initial parameters of the battery. State of health is vital information for the decision if the battery can still be trusted in its function and what performance can be expected.

- SOF ... State Of Function
  The State of Function describes the battery's very ability to deliver the required performance at the moment. This is essential e.g. for automotive applications where the battery is required for critical applications like regenerative braking or servo-braking/steering.

Today these functions are performed by a specially designed discrete circuit like the following:

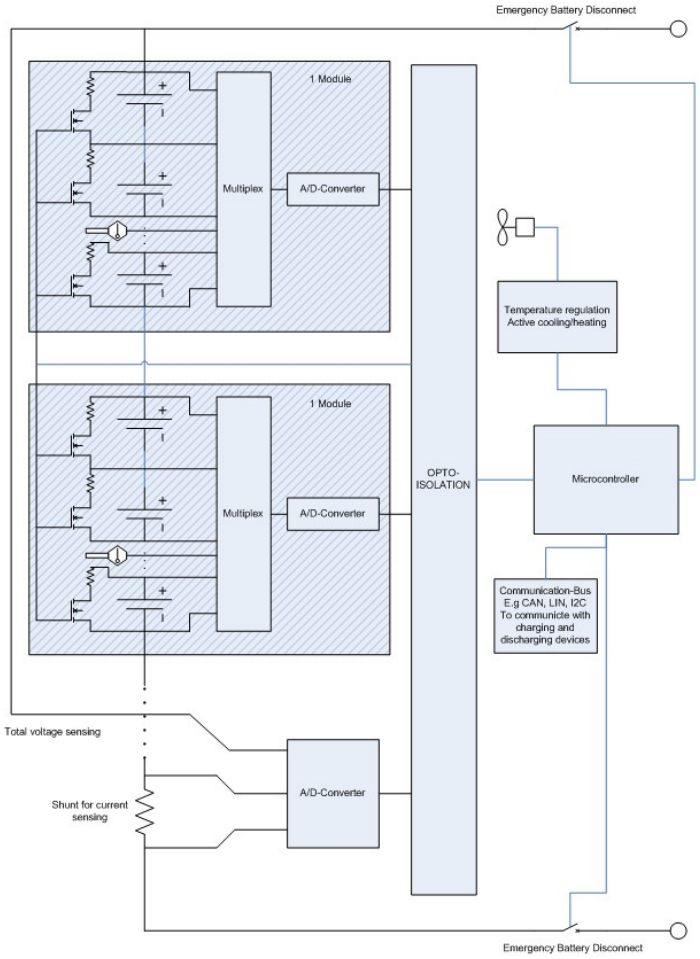

Figure 3.4: Typical Battery Management circuit

For bigger battery stacks (like the ones used in hybrid and electric cars) the battery cells are grouped into modules. Each of the modules uses an A/D converter to measure the cell voltages and temperature. This information is reported back to a microcontroller, which initiates the required actions to keep the cells within their specified parameters or if that is not possible and a safe usage of the battery can't be guaranteed, disconnects the battery from the power system. For smaller battery stacks like the ones used in notebooks or other mobile devices the number of batteries is way lower. Therefore they needn't be grouped into modules. The opto-isolation and the

emergency battery disconnect are generally not implemented. Communication with the main device is normally provided by a special bus called SMBus [5].

3.5 Battery failure

'The performance of Lithium Ion cells is dependent on both the temperature and the operating voltage. The diagram below shows that, at all times, the cell operating voltage and temperature must be kept within the limits indicated by the green box. Once outside the box permanent damage to the cell will be initiated.' [7]

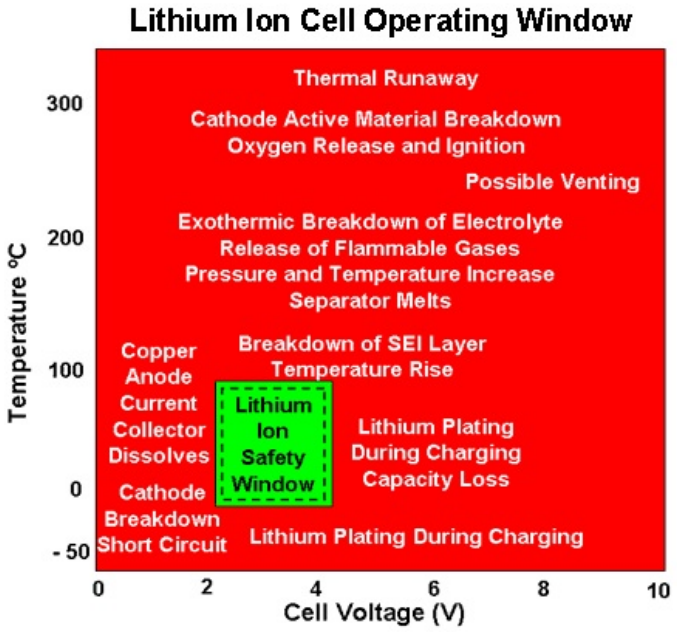

Figure 3.5: Failure conditions for a lithium Cell [7]

In most cases of extreme abuse the battery starts a process which is called thermal runaway.
Thermal runaway occurs when heat output exceeds thermal diffusion. The exothermic reactions that typically lead to such an event are:

- Chemical reduction of the electrolyte by the negative electrode
- Thermal decomposition of the electrolyte
- Oxidation of the electrolyte on the positive electrode
- Thermal decomposition of the anode

- Thermal decomposition of the positive electrode

'It should also be noted that when a seperator melts as a result of the temperature exceeding its melting point, it frequently triggers a large heat ouput induced by an internal shorting' [8]
These processes can lead to the burst/rupture of the cell package and furthermore to the ignition of the remaining cell parts.
In order to maximise the safety of this type of battery a number of testing procedures for the bare cells like:

- Heating test
- Nail penetration test
- Overcharge test
- Crush test

have been established in addition to usage of battery survaillance electronics that prevents most harsh fail states from happening.

4 Battery Balancing

As was discussed earlier battery balancing is the process we use to equalize the state of charge of individual cells within a battery pack. It is part of the battery management hardware and is normally packaged with the battery in a single unit.

Different methods of balancing:
In order to balance batteries a certain misbalance has to be detected first. Physically we know various methods of detecting misbalance

- Voltage based
  The voltage of individual cells is measured either with an ADC or analogue and compared against the average cell voltage.
- Final Voltage based
  Like above but the voltages are only measured at full charge state, which has the advantage that different internal cell resistances don't influence the measurement.
- SOC (history) based
  This method uses data from the battery monitoring system and a mathematical model of the battery chemistry to estimate the state of charge. It is the most complicated but also the most capable model, because it allows balancing at any time and has no problems with internal cell resistance

and compensating this misbalance:

- Passive: The energy from the cells with excess charge is wasted in heat.
  - Charge shunting: While the battery is charged the system monitors the cells. If a cell reaches its full charge state this cell gets bypassed by an external transistor + resistor, so the charge current only affects the remaining cells.
  - Charge bleeding: In this case the system detects the cells with the highest charge and simply burns up their energy in an external bleeding resistor. This can be done at any time.
- Active: The energy is transferred from the cells with higher SOC to those with lower.
  - Flying Capacitor charge distribution: A capacitor is switched between the individual cells of a battery. It picks up charge as it gets attached to the batteries with higher SOC and dumps this charge into batteries with lower SOC. The smaller the voltage difference gets the less charge is transferred. So the efficiency decreases with increasing balance level.

  - Inductive charge distribution: This method uses a transformer (typically a flyback construction) to shuffle charge between different cells. It is more efficient than the capacitive version and can handle high balancing currents.
    * Cell to battery: Charge is transferred from the cells with the highest SOC to the whole battery pack. (fast when few cells are high, low voltage Fet applicable)
    * Battery to cell: Charge is transferred from the whole batter pack to the cells with the lowest SOC. (Fast when few cells have low SOC, single bulk DC/DC converter applicable)
    * Cell to cell: Charge is transferred between individual cells (from cells with high SOC to cells with low SOC). (low voltage per converter, connections don't need high isolation)

4.1 Pack to pack balancing

In applications where more then ten batteries are stacked (typical for electric cars) the batteries get grouped in modules of ten to fourteen cells, which is just below the voltage that is safe for humans to handle. Each of these modules has its own balancing module but there is a need to shuffle energy between different modules to achieve balancing over the whole battery stack. The idea is pretty much the same as for battery to battery balancing and so are the concepts. But there are two interesting approaches that mostly utilize the hardware that is already there:

- Communication: If the balancing circuits in the individual cells are equipped with a means to communicate with each other they can determine the overall average voltage and then balance accordingly.
- Connection of the analogue divider: If an analogue (probably resistive) divider is used to determine the average voltage it is possible not to connect the ends of this divider to the next battery terminal but to the next divider string, thus the divider grows with added modules and the average voltage on one of the resistors is proportional to the actual average over the whole battery.

These two techniques are easy to implement with passive balancing but require a lot more wiring if active balancing is chosen.

4.2 Austriamicrosystems method

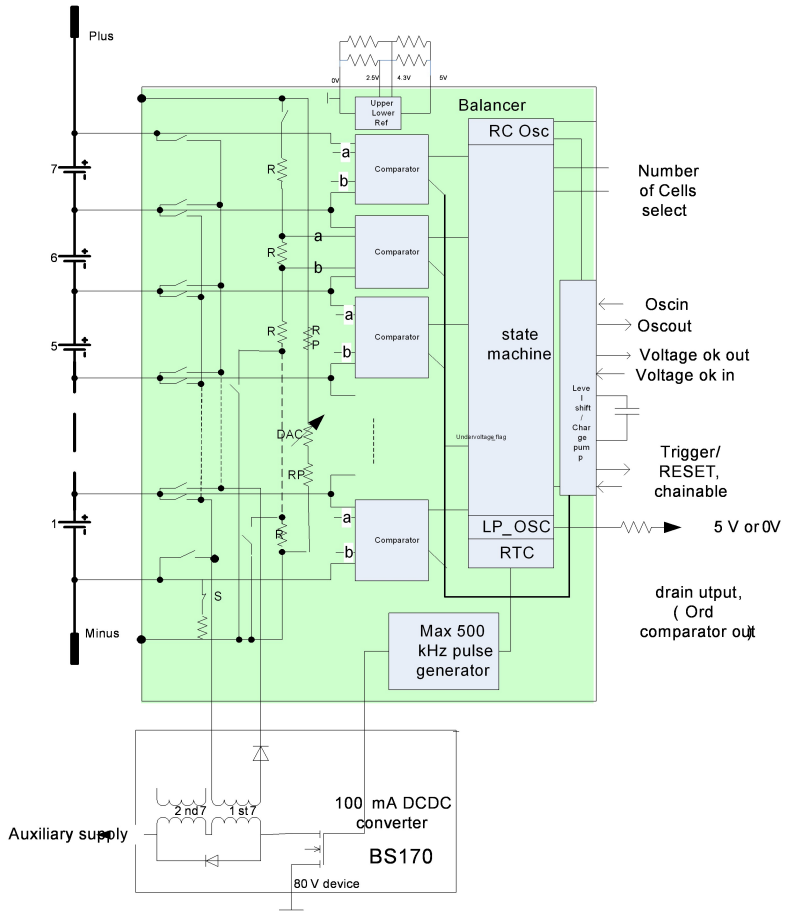

Figure 4.1: Block diagram of the (AS8505) IC

Our method uses analog sensing through a resistive divider (R chain in the middle of the block diagram) and a set of differential comparators to determine the misbalance in a battery stack. For the balancing part the circuit allows the usage of active battery to cell balancing with a flyback converter as well as passive charge bleeding. Both are supported by a network of internal transmission gates seen on the left-hand side. All the components within the green square are to be implemented in an IC

4.3 Basic operation

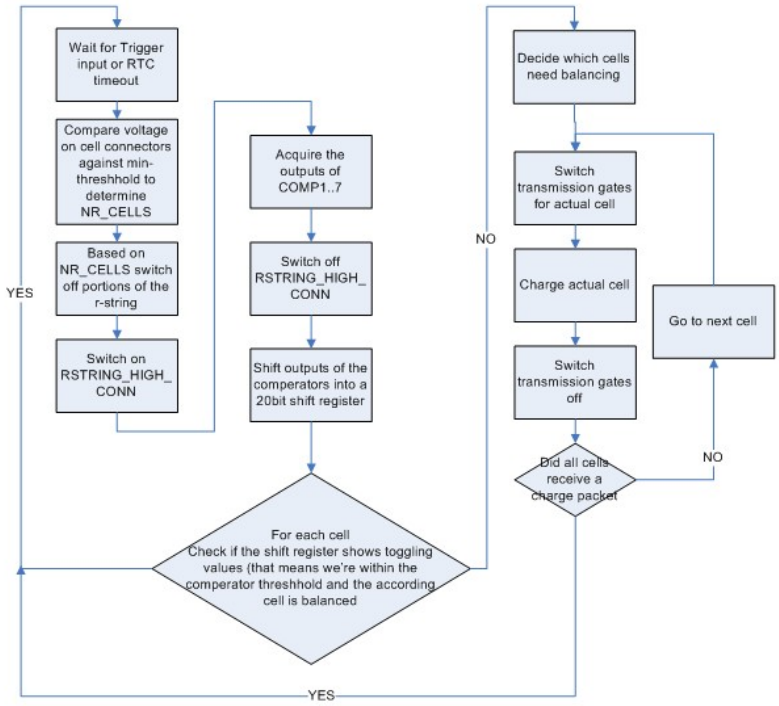

Figure 4.2: Basic operation of the Balancer

The circuit waits (in sleep mode) for an external trigger (provided by a trigger input pin) or the timeout of a built in RTC (which is programmable through external components in the range of a few minutes to a few days) to start its normal operation. This is important to assure very low power consumption whenever the balancing function is not needed. After wakeup it checks the 7 cell connector pins against an internal threshold voltage to determine the number of cells that are connected. According to this number it has to switch off a portion of the resistive divider string to set up the correct division ratio and get the correct average voltage. Now the r-string gets connected to the connection pin and the divided voltage is compared against the different individual voltages of the cells. The digital outputs of the comparators get shifted into a 7x20 bit shift register. After that the r-string is disconnected again to minimise power consumption. The algorithm determining which cells still need balancing simply checks how many 1 (meaning the according cell was below average at the time of measurement) are within the shift register. If the number of 1 is above a certain limit the cell is detected as "too low". After recognizing the cells that still need charging

the state machine goes through a routine for each of these cells which activates the according transmission gates, sends a charge packet (approx 100mA for 1 second) to the cell and then disconnects the transmission gate again. After this routine is done another sample of the comparator values is taken and the cycle starts again until each of the shift registers is filled with a random 1 and 0 combination, meaning the voltage of the cells has reached the average.

4.4 Linking multiple devices

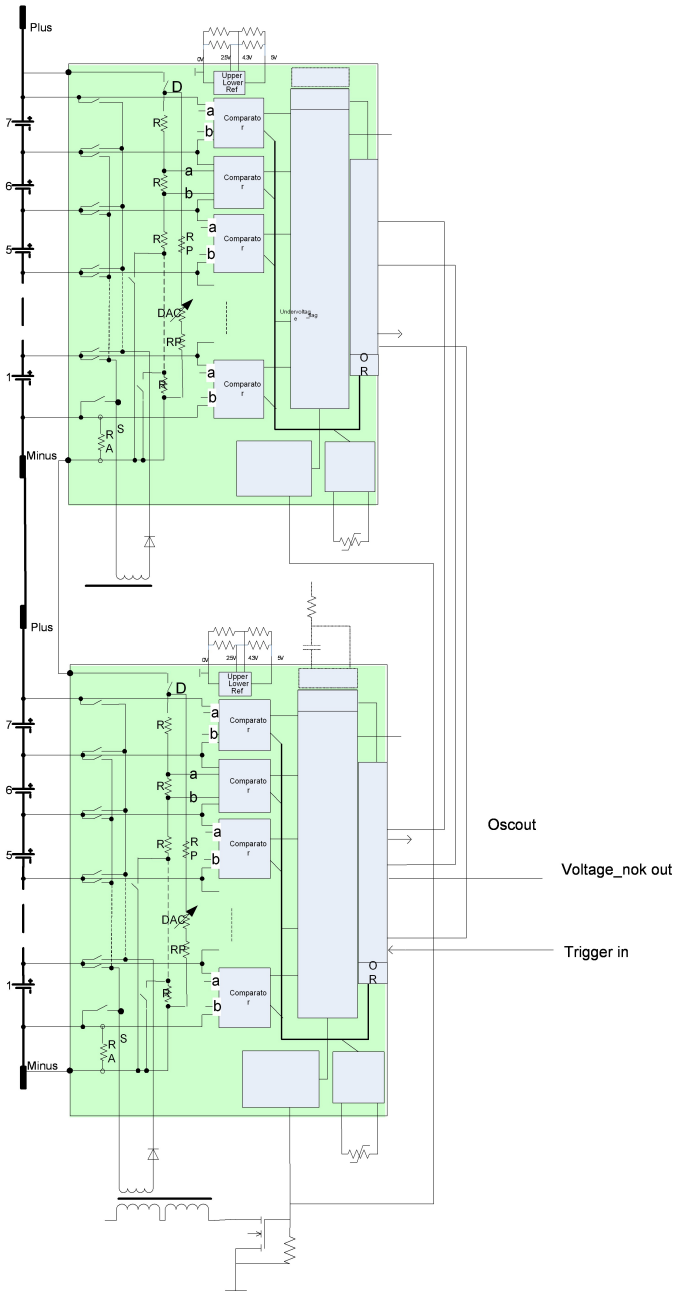

Figure 4.3: Linking of multiple devices

We also implement the facility to link multiples of these devices to allow for battery stacks of more than 7 cells as well as pack to pack balancing. In that case the clock and trigger signals are passed through from one module to another by means of an implemented level shifter. The r strings get connected from top to bottom module to allow the individual modules to detect the actual average voltage over the whole stack. This implies that the r-string has to be able to handle the full voltage of the battery stack (which can be up to 500V) . Therefore we implement a high-ohm resistor that ties the r-string to the local ground potential in order to decrease the risk of excessive ground floating.

4.5 Wiring

The reason why there is an extra chapter on wiring is because it is a significant challenge to design the wiring for special purpose batteries such as the ones used in hybrid or electric vehicles. The main problem is the high voltage of up to 500V dc. In order to make these modules somehow safe to handle they get grouped in modules with about 40V each. These modules are connected serially to form the whole battery. The problem is that the battery does not only need those power lines but also communication and diagnostic lines going into each module. So if these modules use a normal bus topology all these modules have the same potential and therefore have to be isolated against the 500V. This makes for high production costs, and wasted space on isolation. So it is desired to have a means of communication that can be shifted through or daisy chained so that the voltage gap between the modules is only modest. In the case of our balancer we do need to have a connection from the total voltage (500V) to the flyback converter located in each module. This unfortunately means a lot of cabling with high voltage capability, which is very much undesired. Therefore we thought about using the always-present 12V board network as primary power source for the balancing process. This circumvents the necessity for a high voltage line and allows us to have a dual line voltage bus from which each individual module is fed.

5 Battery Balancer Prototype

5.1 Approach

As one can see in the schematic 11.1 the battery voltage of each cell is fed through an inverting OpAmp with an offset of 5V. This transforms the differential cell voltage between 2.8 and 4.2 V into a single ended output voltage between 2.2 and 0.8 V. The same procedure recurs with the voltage that is derived from the resistive voltage divider string. The reason why we don't simply use the voltage across the lowest resistor is that the length of the r-string can be shortened with the n-fets at the bottom, cancelling out the low resistors. This gives us the possibility to have battery packs with a varying number of cells. The level shift is necessary to accommodate for a comparator that can work on a 5 Volt supply while remaining a constant positive offset on the input of the OpAmps so that they don't have to accept signals that go near their power supply rails. Transmission gates at both ends of the string allow to disconnect the string totally (while in charging mode) and to de-float the string in respect to the absolute cell voltage. The single ended battery voltages as well as the outputs of the comparators get forwarded to the microcontroller (which represents the digital logic of the silicon implementation). Based on the outputs of the comparators the microcontroller decides which cells need to be balanced, sets the transmission gates accordingly and then starts clocking the pwm (pulse width modulation) output which drives the MosFet of the flyback converter. After each underbalanced cell has received a charge of approximately 100mA for one second the measurement starts again. While performing all those operations (which in the long run should be implemented on chip) the microcontroller also takes measurement of the single battery voltages as well as the floating level on the upper and lower portion of the r-string. The resulting information is displayed on a character LCD which is attached to the microcontroller for demonstration purposes. Since an option to stack multiple of these demonstration boards just like the real chips later on should be available, the demonstration boards are only connected to the specific portion of the battery stack they are foreseen to balance, while the r-string can be tied to the r-string of the next board. Topmost and bottommost r-strings are then connected to the end terminals of the battery. This allows not only to balance the cells within one demonstration board (7 cells) but a whole battery stack with a nearly infinite number of individual cells. In order to synchronise the boards the clock and trigger signals have to be forwarded. This is done by optocoupling the signals at the input so they get shifted to the relative offset of the specific balancing board. It is assumed that this functionality may later on

be implemented by a level shifter combined with a charge pump that shifts the level approximately 3.3 volts over the supply rail in order to have a cmos compatible input for the next stage.

5.2 Component selection

Input stage (OpAmps): The input opamps were chosen for their ability to handle the nominal supply voltage of 30V as well as a common mode voltage that can go as high as the supply rails. They also sport a very low input bias current, which is very important as not to alter the measured voltage off the battery due to losses over the series resistors connecting to the battery. The input offset voltage had to be very low to decrease the error on the output. All of the used OpAmps are of the same type (LT1673) in order to ease the development, although the OpAmps in the middle don't actually need rail to rail capabilities. The opamp is configured as an inverting amplifier with an offset of 5V on the positive input.

During testing the OpAmp that derives the voltage from the r-string showed instability on its output (in form of a 100mV sinus ripple overlaid with the dc voltage) and was therefore replaced by a TL062 from Texas Instruments. It turned out that the opamp wasn't stable at a gain of 1. This was described in the opamps's datasheet but overlooked during design.

Resistors: All resistors used in dividing an amplifying stage are 0.1% precision resistors in order to achieve the necessary total accuracy of $\approx 5mV$.

Comparators: As the OpAmps shift the voltage of the battery stack to within a normal TTL level we could use the AS1972 rail to rail comparator to compare the individual cell voltages with the average per cell voltage to determine which cells need balancing.

Microcontroller: The whole digital logic of the circuit is implemented in an ATmega1280 AVR microcontroller. It works through a software flow shown in figure 5.8. Its two main tasks are the detection of the unbalanced cells (and subsequent charging of those) and the display of the individual cell voltage on a display for the user to track the balancing progress.

LCD: A classic 4x20 character display was chosen to display the status and charge parameters. It was the best compromise between ease of use and interaction with the user.

Transmission Gates: The MAX4690 transmission gates do mainly serve the purpose of distributing the charge impulses to the cells that need charging. They do always work in pairs to connect the + and − connector of a single cell to the secondary coil of the flyback transformer. Two of the transmission gates are there to connect/disconnect the r-string to target and to change it from floating into non floating mode (if the float levels are too big).

Switch mode converter: We are using a flyback converter to transfer energy from either the whole battery stack or an auxiliary supply to an individual cell. There are a few different topologies which were evaluated during design. Each of them has its

specific advantages and disadvantages. For simplicity of use we decided for the flyback topology.

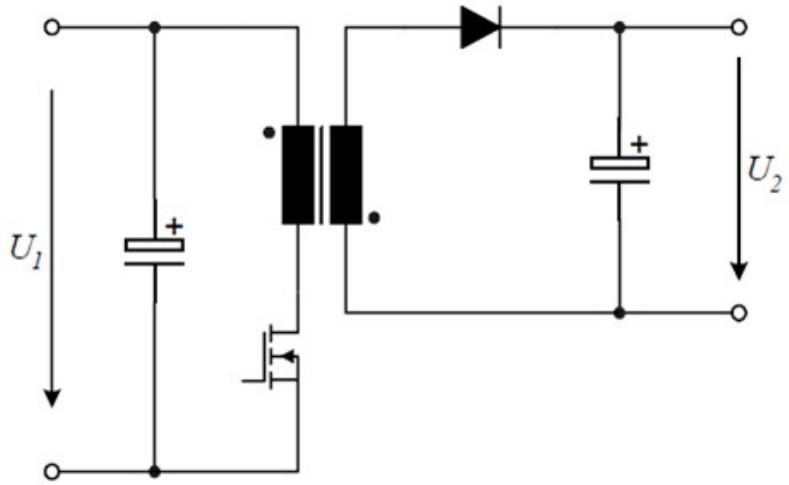

Figure 5.1: Basic topology of a flyback converter [11]

This type of converter stores energy in the magnetic field while the switch, or in this case fet, is turned on and then releases the energy into the secondary side (through the forward diode) when the switch is turned off:

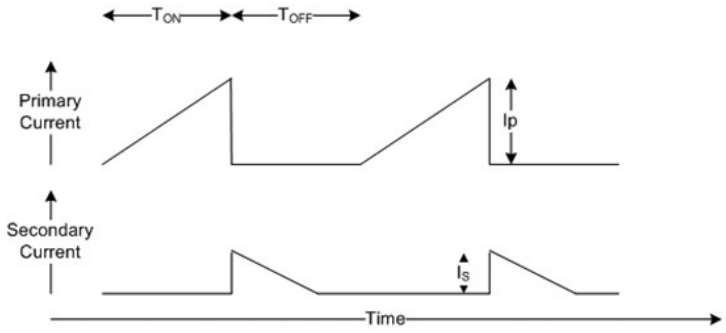

Figure 5.2: Currents in a flyback converter [12]

5.3 Calculation of the magnetic core

We start out with some basic parameters for the secondary side:
The voltage of the battery is between 3.8 and 4.2 and 4V are used for this calculation

$$Usec = 4V(VBat) + 0.7V(VDiode) = 4.7V$$

We also agree on an average charging current of 100mA

$$Isec = 0.1A$$

and

$$Psec = Isec * Usec = 0,47W$$

with a typical efficiency of 75% we need

$$Pprim = \frac{Psec}{\eta} = \frac{0,47}{0,75} = 0,62W$$

the typical supply voltage for the transformer would normally be

$$Vprim = 12V$$

The switching parameters are as follows

$$\begin{aligned} f &= 200kHz \\ dutycycle &= 50\% \\ ton &= 2,5\mu s \end{aligned}$$

$$\begin{aligned} Uprim &= Lprim * \frac{\Delta I}{\Delta t} = Lprim * \frac{\hat{Iprim}}{ton} \\ \hat{Iprim} &= \frac{Uprim * ton}{lprim} \\ Wprim &= \frac{Lprim * \hat{Iprim}^2}{2} \\ Pprim &= Wprim * f \rightarrow \\ Pprim &= \frac{Lprim * Uprim^2 * ton^2 * f}{2 * Lprim^2} \rightarrow \\ Lprim &= \frac{Uprim^2 * ton^2 * f}{2 * Pprim} \\ Lprim &= 143,62\mu H \end{aligned}$$

And the secondary inductivity:

$$Lsec = \frac{Usec^2 * toff^2 * f}{2 * Psec}$$

Assuming that the discharge cycle takes the same time as the charging cycle we get:

$$Lsec = 29,37\mu H$$

We chose a Kaschke EP 7 [13] core as first candidate. This transformer is available in an SMD package which will fit the narrow space available but has enough magnetic material to transfer the necessary energy. It also supports the used switching frequency.

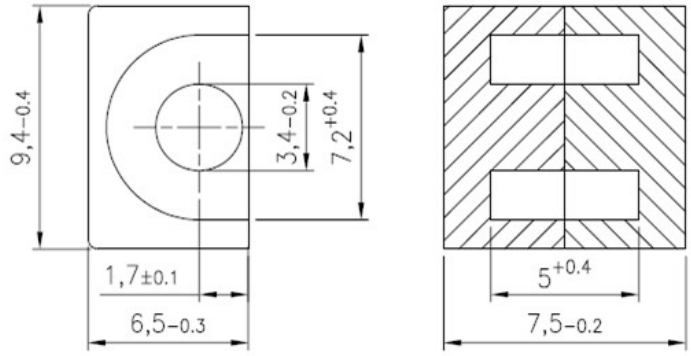

Figure 5.3: Kaschke transformer core

The data of the transformer are as follows:

Material: K2008
Al: 1680nH
Bmax: 500mT
Losses at 200khz smaller than 3%

With these data we can calculate:

$$\begin{aligned} N &= \sqrt{\frac{L}{Ai}} \\ Nprim &= 9,47 \approx 10 \\ Nsec &= 4,28 \approx 4 \end{aligned}$$

During the first tests with this transformer we found the L-values to be varying widely. Some of the hand wound transformers worked, others didn't . So we searched for another solution and found it in the Wuerth ER 11/5 [14]. This transformer has 6 pre wound coils which can be combined to fit our needed inductance values.

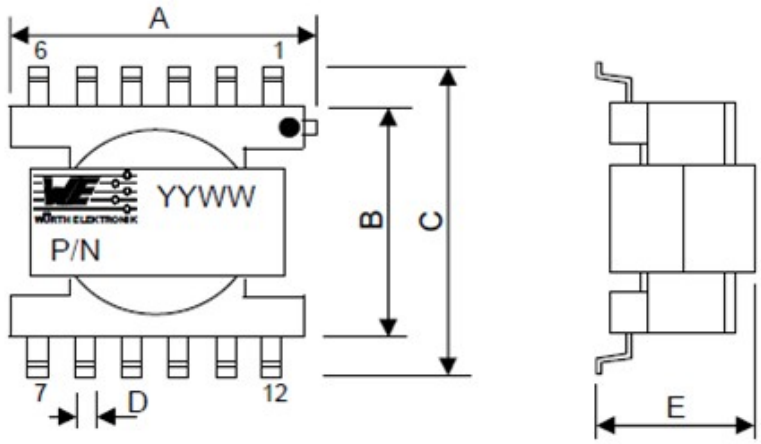

Figure 5.4: Wuerth transformer core

The Wuerth WE-Flex Designer [15] allows calculation of the correct transformer values and winding configuration. The following data were used as input for the calculation:

$Uin_{min} = 6V$ $Uin_{max} = 18V$ Uout = 4,2V Iout = 0,1A fsw = 250kHz
For this configuration the program suggested a 1:1 winding combination of the six coils using three coils per side in seriesas seen in figure 5.5

This yields the following electric parameters (figure 5.6)

We did a couple of test runs with this transformer to determine the optimal pwm duty cycle for the input voltage range on a normal 12V car supply line (which is between 6V and 18V due to different load conditions).

In this diagram one can see that it is recommended to change the duty cycle according

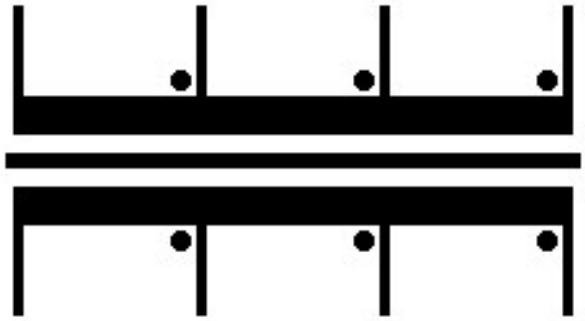

Figure 5.5: Winding configuration of Wuerth transformer

Core:	ER 11/5	Order Code:	749 196 111
Turns Ratio:	3 : 3	Duty Cycle:	0,45
$I_{in,max}$:	0,217 A	$I_{out,max}$:	0,2 A
$I_{in,rms}$:	0,131 A	$I_{out,rms}$:	0,135 A
Lprim:	246,6 µH	$I_{out,ripple}$:	0,038 A
		Pout:	0,42 W

Figure 5.6: Calculated parameters of Wuerth transformer

to the supply voltage. Otherwise we would have to choose the 25% duty cycle to not get into trouble with excessive currents at high voltages, which would determine that the charging current at the nominal voltage of 12V was very low.

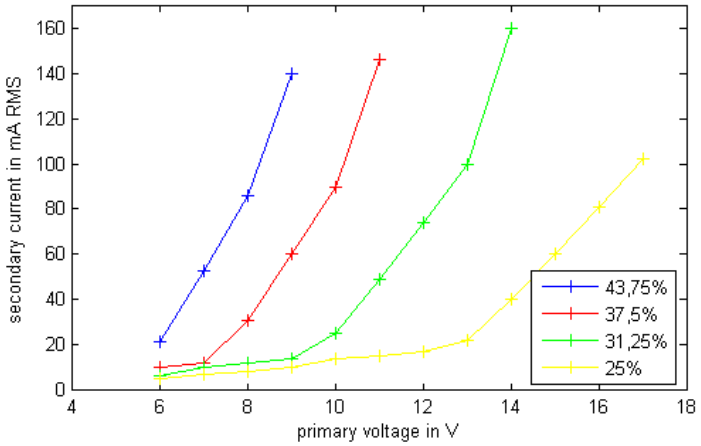

Figure 5.7: Output current vs. input voltage for different duty cycles

5.4 Software

The software is written in ANSI-C and compiled with the GCC and AVR-libc as build environment. The Atmega 1280 microcontroller has enough flash as well as sram memory to fit even bigger c-routines. The software starts out displaying a welcome page and the firmware version on the character lcd which is interfaced through a software only driver from Peter Fleury [9]. Then it initiates a timer to call an interrupt every 100ms which reads the individual cell voltages through the integrated adc and displays these as well as some generic status information on the display. The main program goes into an infinite while loop which processes the sates of the voltage comparators, decides which cells need to get balanced and then subsequently switches on the necessary transmission gates and charges those cells. For ease of use a small menu was added which allows to start and stop the balancing process as well as change some system parameters, like charging time per cell and duty cycle for charging.

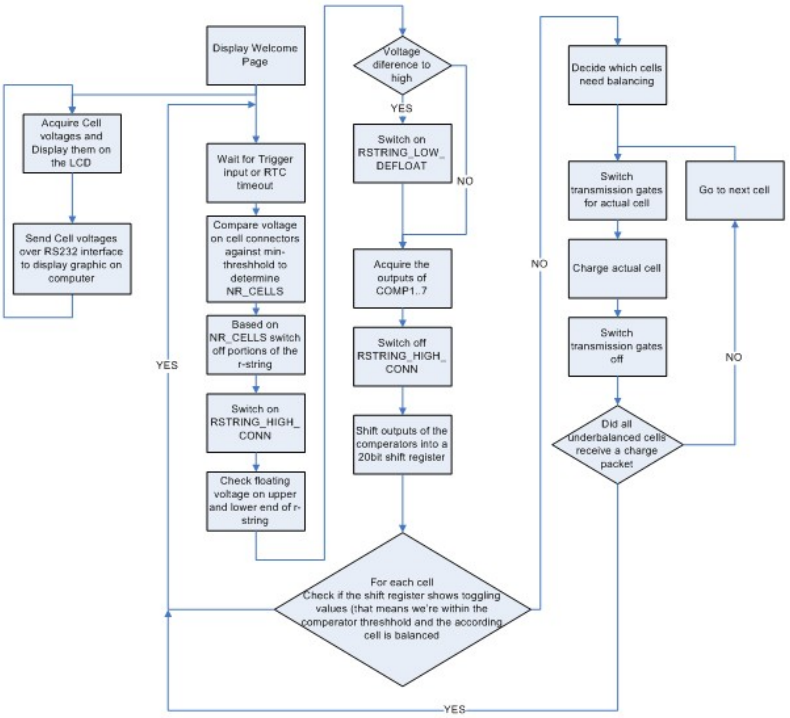

Figure 5.8: Balancing prototype flowchart

6 Battery Monitor

6.1 Approach

The battery monitor is a tool to accurately monitor the balancing in progress and verify the function of the prototype as well as the final ASIC. It is also a proof of concept for the AS8510 circuit to demonstrate its ability to measure single battery cell voltages with an accuracy <1mV.

The circuit will also be used for battery characterisation in combination with an active load (discussed later on) and a source to recharge the battery. The idea is to test battery balancing in the three different load conditions (charging, standby, discharging) of a battery. We also would like to verify the total effective capacity before and after balancing and the energy investment versus capacity gain of a balancing process. This should be especially interesting compared to a passive balancing process.

The idea was to build a voltage measurement tool that could measure a battery module of 12 cells with 4.2 V each simultaneously while maintaining an accuracy of more than 1mV. The austrimicrosystems AS8510 was the ADC of choice. It is primarily designed for 12 V batteries but can be adapted for a wider voltage range. The primary advantage of this chip for our purpose is that you can use it without internal amplification and therefore gain the advantage of a negligible input offset. In order to use that feature we had to translate the cell voltages to a measurement voltage suited for the AS8510 (which is about 1V). We decided to use a precision resistive divider to divide the voltage of each cell into about 0.5V measurement voltage. Then we used one AS8510 per 2 batter cells and connected the local ground of the AS8510 with the − pin of the lower battery cell. This means each ADC runs with a different ground potential. Galvanic couplers from the AD iCoupler© series were used to shift the potentials of the individual measurement paths to the microcontroller in use.

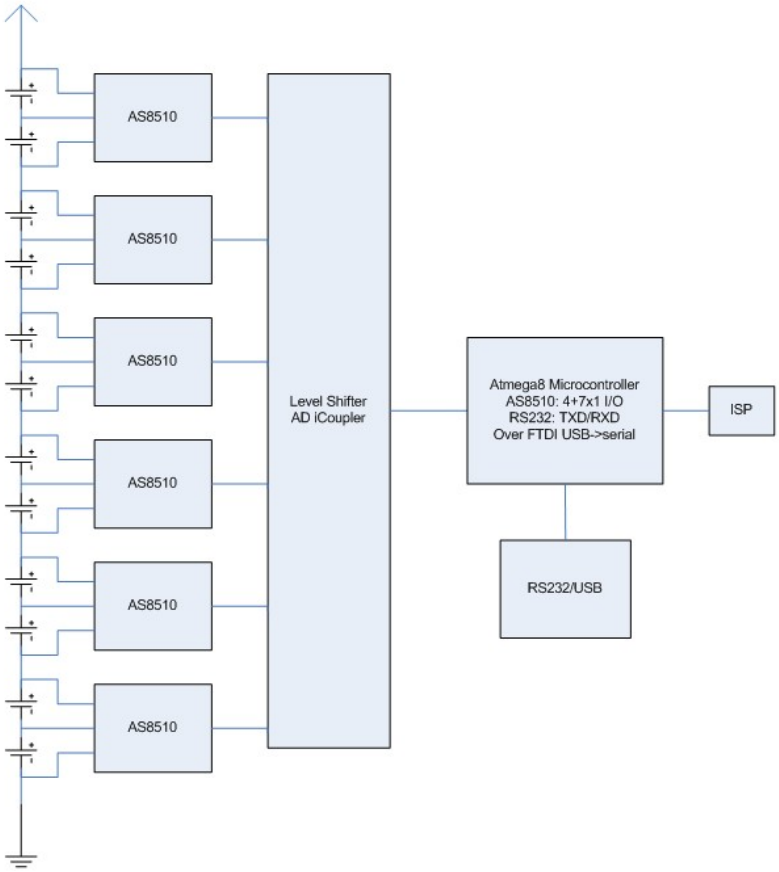

Figure 6.1: Battery Monitor Block diagram

This microcontroller responds to a serial input (provided by an USB → serial converter). On request it checks the individual cell voltages and reports them back via the interface. The AS8510 allows the connection of PT100 temperature sensors to collect temperature data from the cells.

6.2 Component selection

ADC: The AS8510 was chosen for its very low input offset voltage as well as the required resolution (16bit). It has two differential inputs which are connected to the respective battery cells via a resistive divider. It also features two inputs for ratiometric temperature measurement. (in this mode one pin is connected to a known resistor and

the other one to a PT100. The current source for these pins is internal and can be configured).

Galvanic isolation: To connect the signal lines of the six ADCs to a single one leading to the microcontroller we had to build isolation gaps. This is necessary to shift the logic levels to the required ground level. The AD iCoupler© series features a high frequency magnetic coupling system integrated on a chip as well as a low power isolated transformer to power the ADCs. We chose the ADUM1100 and the ADUM5402 to transmit a total of 5 logic lines and power the devices from the USB port to not draw more than the necessary measurement current from the battery.

Microcontroller: The Atmega 8L was chosen for its ability to work at 3.3V (like the ADCs and the FTDI chip). It features the necessary ports to communicate to the AS8510 as well as a serial interface for connectivity to the Pc.

USB to Serial: The FTDI FT232RL was chosen as USB→serial conversion chip. The company provides drivers for all common operating systems which allow it to be detected as a virtual com port. This makes it easy to interface with any common pc program that can handle serial communication (in our case Labview©) The chip itself only needs a handful of decoupling resistors and a sub connector to work properly. It is therefore perfectly suited to get rid of the RS232 port on the PC side, which is not present in most modern computers, and still use the benefits of the simple interface in the microcontroller firmware.

6.3 PCB-considerations

On the pcb there is a copper free space between the secondary and the primary side of the couplers. We didn't want to have any traces passing over this gap. In case of a short circuit on the battery side the rest of the board as well as the pc connected to it stays well protected. There are also a few 100nF decoupling capacitors near the ADCs to filter out spikes in the supply voltage (produced by the switch mode power transport within the converters)

6.4 Decoupling

In the first tests the supply voltage coming out of the 3.3V regulator did have a huge ripple of about 0.4VRms. We inserted another 3.3uF decoupling cap in front of the regulator and a 10uF cap directly after. It also turned out that the microcontroller needed an extra decoupling cap to not suffer from the voltage spikes introduced by the iCoupler© devices. We placed an additional 10uF as well as a 100nF cap directly beside the microcontroller, which solved the problem completely. We also added 100nF

caps for the vreg and agnd lines of the AS8510 to resolve noise issues during conversion.

6.5 Firmware

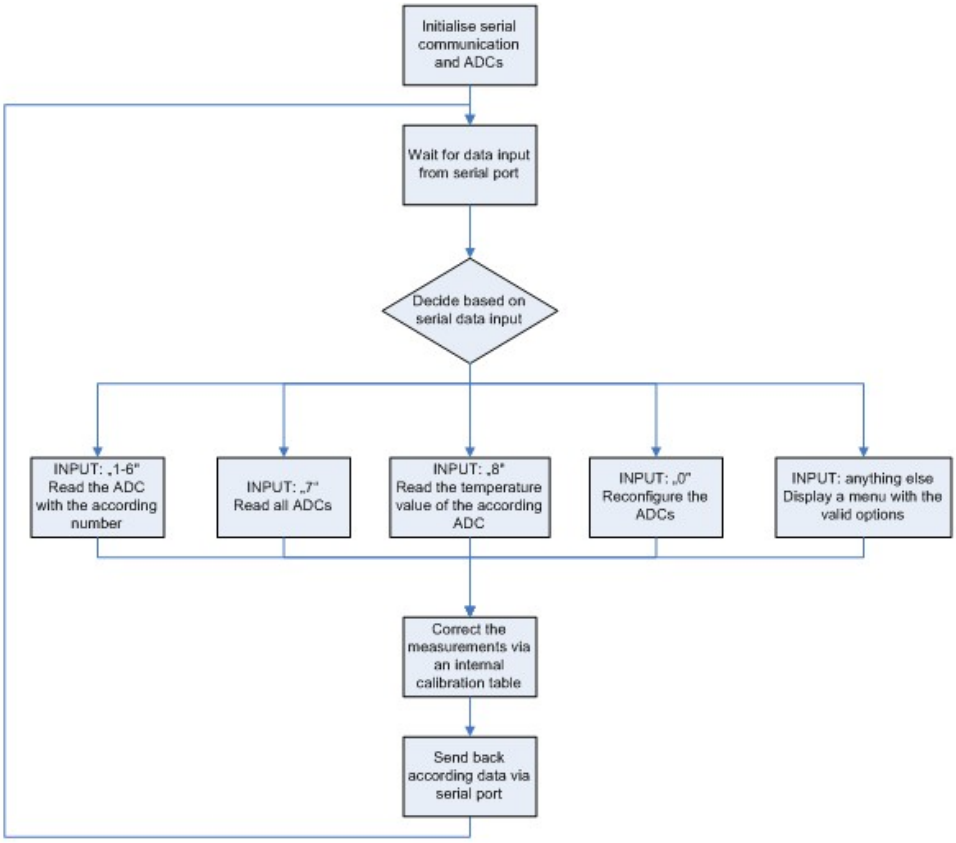

Figure 6.2: Battery Monitor Flow chart

The software was again written in ANSI-C using the same toolchain as with the balancing prototype. The state machine runs through an infinite loop recognizing the symbols sent from the PC through the serial port, then reads back the according ADC values and sends them via the serial port.

6.6 Communication problems

During the test of the developed firmware it was becoming obvious that there was a problem with communication to the ADC. Whenever data was requested with a delay between requests of less than 100ms the answer of the chip was random. After debugging the SPI Interface with a logic analyzer it was found that the SDO line keeps its last status after the chip is deselected for another 100ms so if the last transmitted bit (from the ADC to the microcontroller that is) was a high bit, this status would remain on the bus for 100ms. On the Logic Analyzer we can clearly see that:

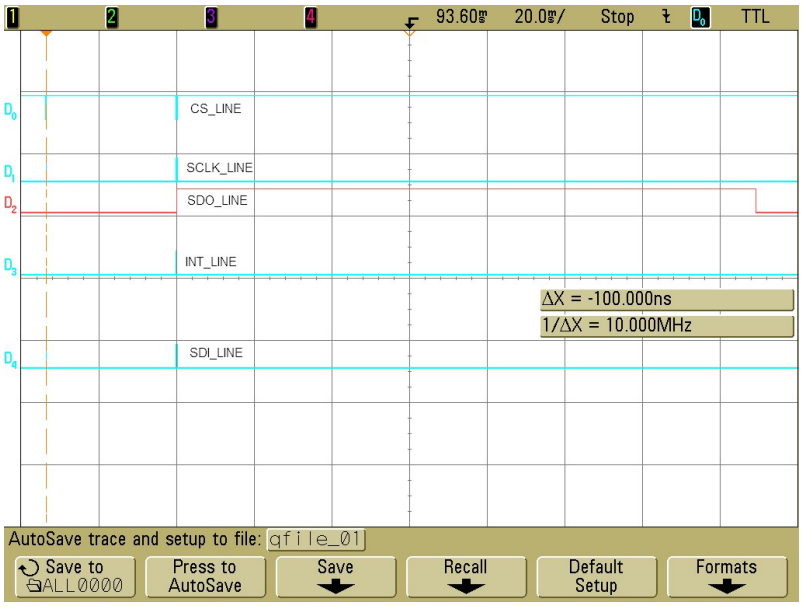

Figure 6.3: Communication problems due to hanging SDO line

Since all 6 ADCs are connected to the same bus (with an OR-gate) this high state disturbs data transmission from the other (following) ADCs. I figured out a software workaround by reading a system status register which has a 0 as its last bit. Therefore the bus is resuming low voltage after transmission and not blocking the other ADCs anymore:

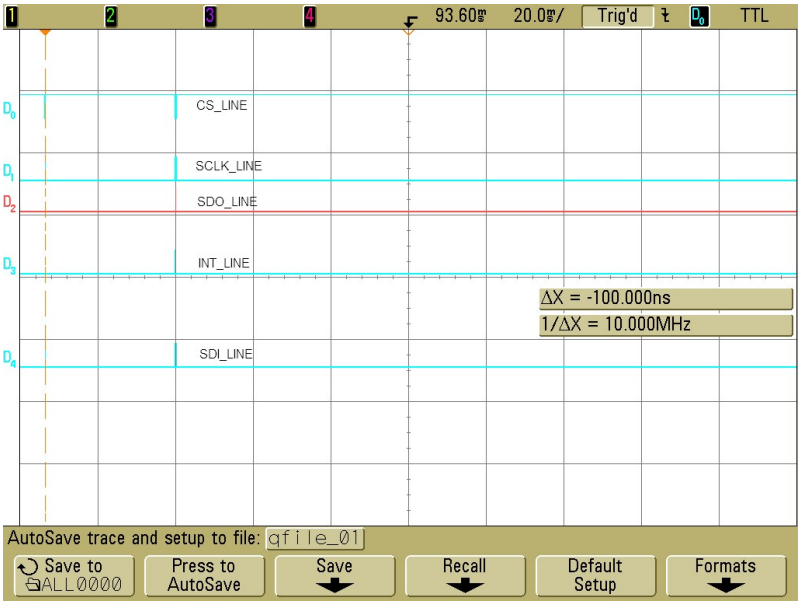

Figure 6.4: Communication problems solved

After successfully trying this solution we did additional testing on the communication lines, which revealed that the output of the AS8510 did in fact enter TRI-state status, but the voltage on the line connected to the iCoupler© remained in high state due to the very high input resistance of these devices. Connecting a $470K\Omega$ resistor from the SDO line to local ground solved this problem.

6.7 PC-software

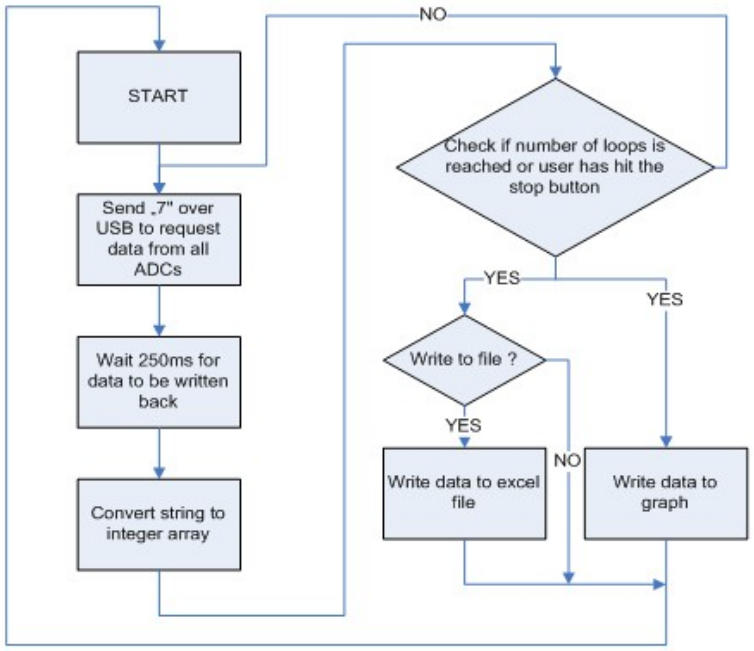

Figure 6.5: Battery monitor software flowchart

The Pc software was created in NI Labview©. Its main goal is to read the voltage values of the batteries connected to the Battery Monitor and display them in a graph. It also features a function that writes the taken values to an excel file for later analysis. Communication takes place via a simple RS232 protocol. The PC-software sends a single character to request data, then waits for approximately 250ms and reads back the RS232 buffer. The received string gets translated to integer numbers and put out on a graph.

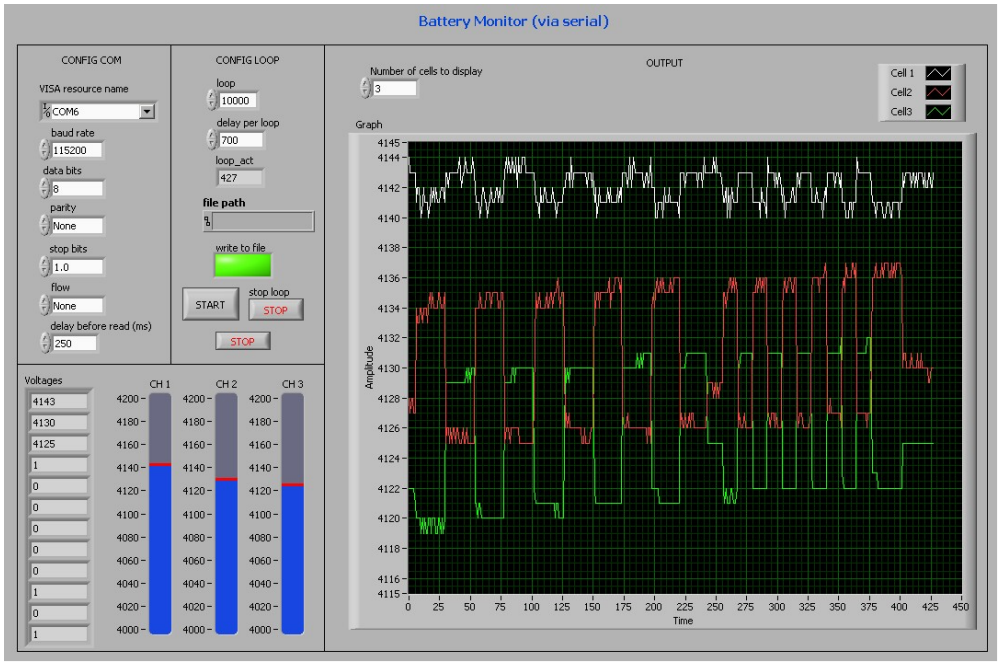

Figure 6.6: Battery monitor software

It was found that timing was a major issue with the Labview© software. Although the delay per measurement was set up to allow for one measurement each second the actual time between measurements drifted quite a bit. We found a way to circumvent this problem by reading the Windows timestamp while running the program and waiting for a change in the "second" variable to start with the next measurement. As an additional measure we also print out the timestamp to the generated excel files.

7 Active Load

7.1 Approach

The idea was to test the balancing under typical operating conditions, which means we have to simulate three different states: charging, standby and discharging. We wanted a load that would stress the cells with their rated power. So in our case as we are using 12 Li-Polymer cells with 4.2V each and a maximum discharge current of 20A that means:

$$P_{discharge} = 12 * 4.2 * 20 = 1008W$$

So handling a total of roughly 1kW of discharge power over a discharge period (in this case a few minutes) has to be guaranteed.
The decision between linear regulated or pwm-regulated load was in favour of linear regulation. It has the advantage of a way better EMC performance and allows smooth load regulation.

The circuit basically uses a pwm signal which is then filtered by a lowpass filter and passed through an OpAmp to convert the input voltage into load current:

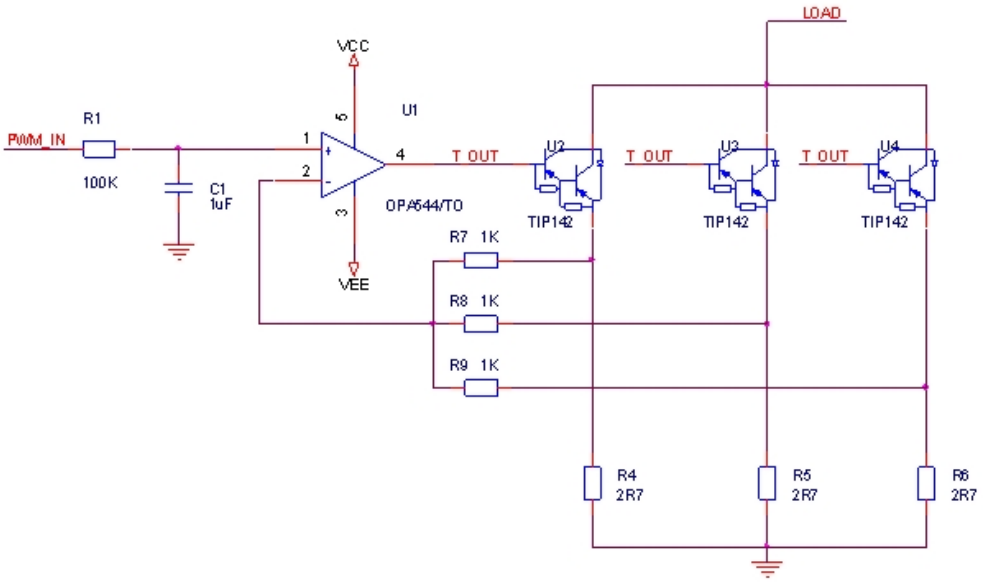

Figure 7.1: Active Load Current regulation schematic

The feedback is closed via an average building circuit (built with resistors R7,R8,R9). Therefore the total current is proportional to the average current per transistor times number of transistors (which in our case is 20). The emitter resistors serve a second function which is to compensate for bias point drift (to stop thermal runaway) and part tolerances (mainly in the current gain). Simulation shows that the relation between pwm duty cycle and current flowing into the device can be diagrammed as follows:

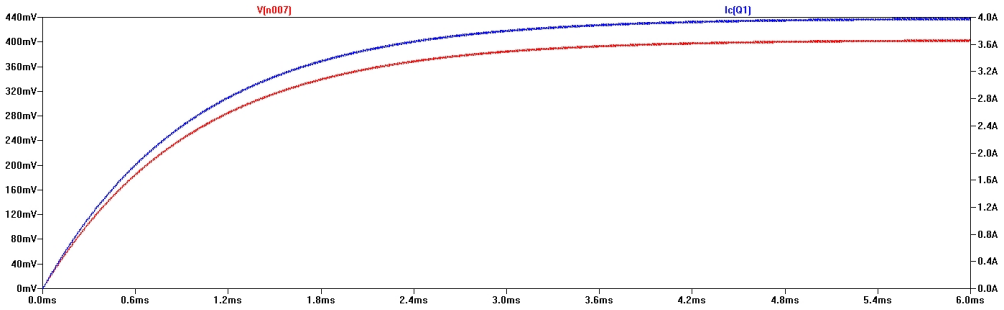

Figure 7.2: Voltage at input of the OpAmp and current through the load path @ 12.5% duty cycle simulated in LTSpice

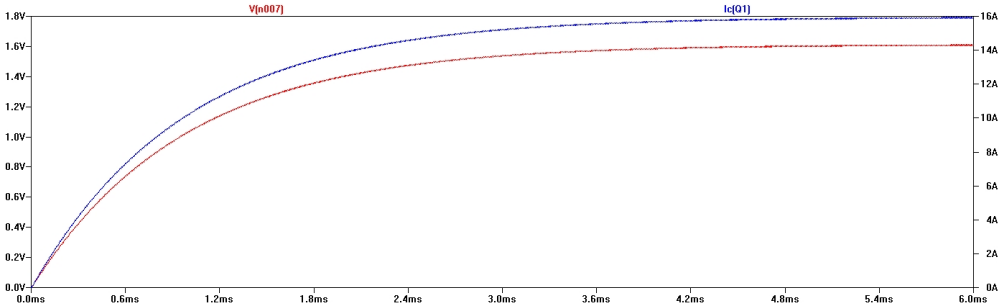

Figure 7.3: Voltage at input of the OpAmp and current through the load path @ 50% duty cycle simulated in LTSpice

We can easily see that the relation between pwm duty cycle and current is pretty good if we don't change the duty cycle faster than the lowpass filter can settle. In our case, where we only have low dynamics in the load, this doesn't create any problems.

7.2 Component selection

Transistors: We decided for the ST TIP142 Darlington power transistor to handle the power dissipation. They can dissipate up to 125 Watt each, have a high current gain, which makes them easier to control and they are not too expensive.

Cooling: The transistors have a minimum junction to case resistance of 1K/W their maximum operation junction temperature is $150°C$. The heatsinks we chose have a case to ambient resistance of 1.2 K/W creating a total resistance of 2.2 K/W. If we assume the ambient temperature to be around $30°C$ that would leave

$$P_{diss} = \frac{150 - 30}{2,2} = 54W \tag{7.1}$$

This means in order to achieve the 1KW of total power dissipation we need

$$N = \frac{1008}{54} = 18,9 \approx 19 \tag{7.2}$$

transistors with heatsinks. In our case we installed a total of 20 transistors to allow for non idealities.

OpAmp: Since we have to drive 20 transistors with a base current of up to 20mA each we decided for a single high power OpAmp. We found the OPA544 from Ti© to be ideal. It can deliver a total current of up to 2A and has internal short circuit and overheat protection.

7.3 Mechanical construction

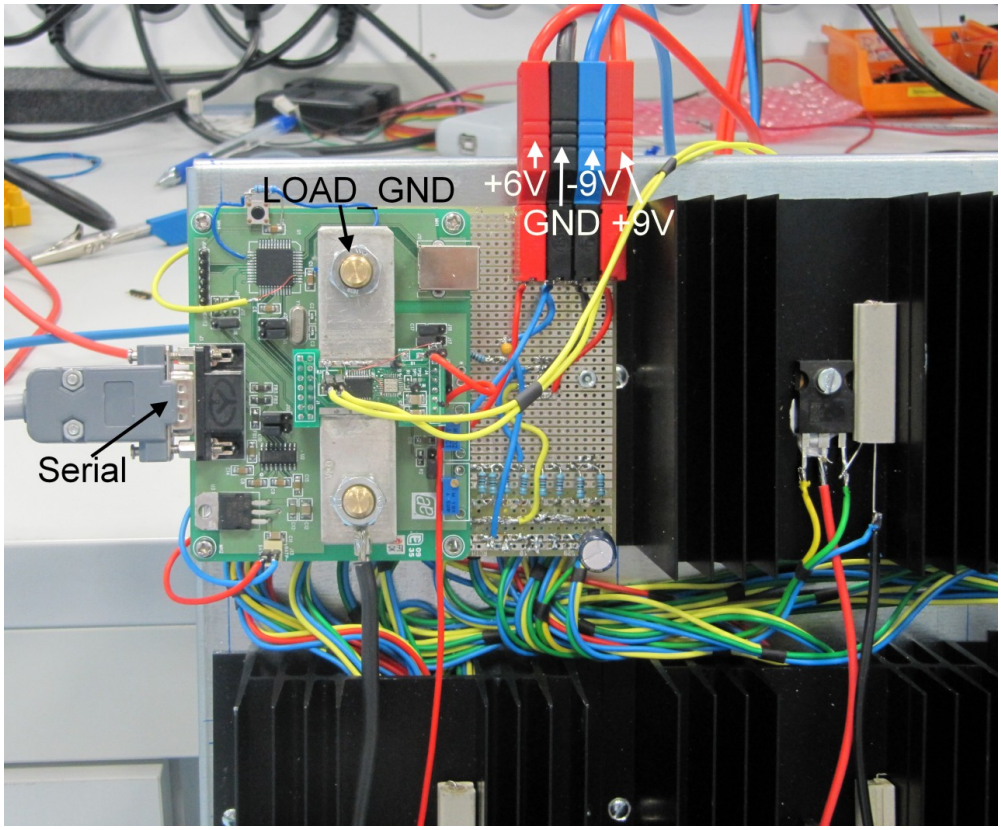

Figure 7.4: Active Load connection diagram

The pwm signal is generated by an AS8510 demo board. This demo board was constructed to demonstrate the AS8510s ability to monitor current and voltage of a standard 12V car battery. It features a high side measurement system (meaning current is measured on the + pole of the battery) built from the AS 8525 and the AS8510 as well as a microcontroller from microchip that reads out the data and communicates it via the RS232 interface. Because this setup is limited to a maximum of 18V we had to rewire the measurement board for low side measurement. We removed the AS8525 high side chip and soldered the shunt resistors directly to the AS8510. Then we installed a new voltage regulator for supply, a reset circuit for the microcontroller and a resistive voltage divider for the voltage measurement path. At last we added a new cable to connect the PWM signal from the microcontroller to the low pass filter.

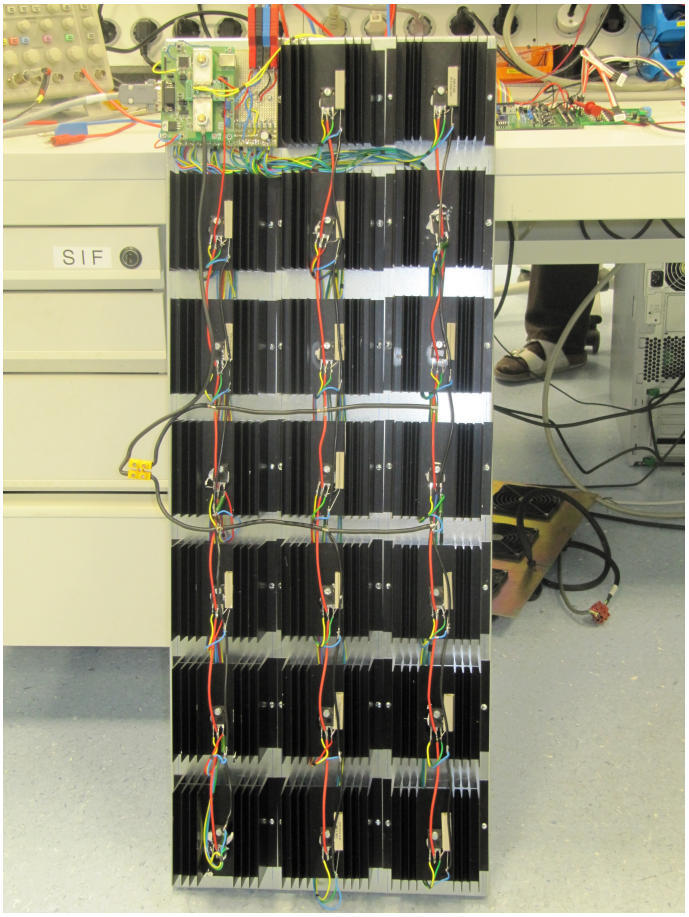

Figure 7.5: Picture of the mechanical construction

All 20 heatsinks were screwed to a common aluminium plate which also houses the OpAmp circuit and the AS8510 demo board. Individual wires were connected from the base of each transistor to the output of the opamp as well as from both ends of the shunt resistor to the input of the opamp in order to achieve a current free measurement path.

8 Charger

8.1 Approach

The charger was constructed in order to allow testing of the balance algorithm while charging. I wrote a script which charges batteries with an HP 6030A System Power Supply.

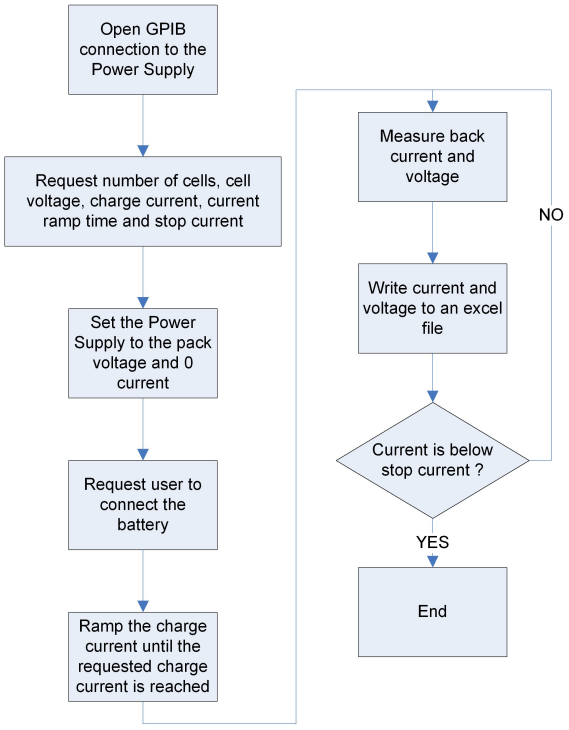

Figure 8.1: Battery charging VI flow chart

The software sets up the power supply, configures the voltages and currents according

to the number of cells and the maximum charge current. Then it slowly increases the current delivered to the battery until it reaches the defined charge current. Afterwards it does a CC / CV charge and after reaching the CV part measures back the current drawn by the battery to determine the full charge point. Full charge current is also programmable through the interface.

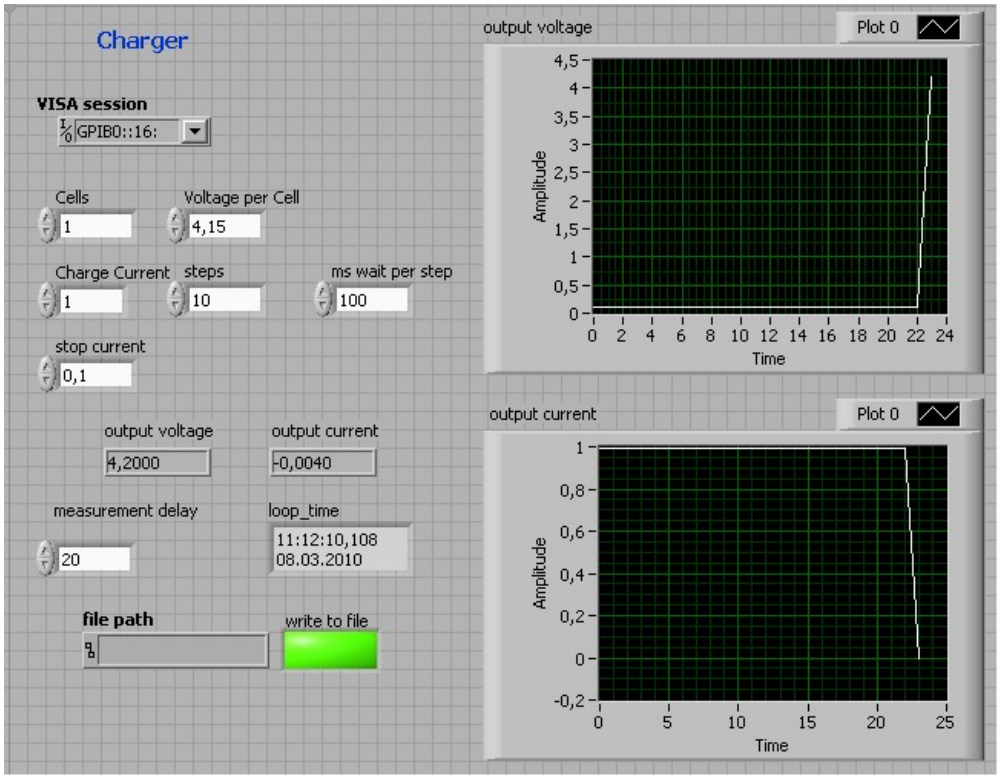

Figure 8.2: Battery charging VI

During evaluation it became obvious that the power supply short-circuits its outputs once the voltage is set to zero. So I had to come up with another way to terminate charging at the end of the charging cycle.

I found that the easiest way to do this is by reducing the current to 0 and therefore forcing the power supply into current control mode so the voltage on the output of the supply is then determined by the connected battery.

This system works quite nice but has one slight disadvantage. Although the current on the power supply is set to zero there seems to be a small leakage current running from the battery into the supply which gradually discharges the battery. But since this software is only used for testing and the effect is very small it can be neglected.

9 Evaluation

To evaluate the battery monitor as well as the battery balancer a series of tests were done.

All measurements use

- The battery monitor (discussed above) for monitoring each individual cell
- The battery balancer prototype
- The active load to simulate discharging
- The HP6030A with my Labview program to charge the battery pack
- One or several 2100mAh 3-cell LiPO pack from Sehan Enertech

The tests done are the following:

- Complete charge of battery with U/I graph
- Complete discharge of battery with U/I graph at several discharging rates
- Misbalance battery with external resistor
- Balance battery while battery is in idle state
- Balance battery while battery is being charged
- Balance battery while battery is being discharged.
- Balance battery at a certain SOC, then charge it and discharge it to the same SOC, check if the battery is in a balanced state or how much misbalance has occurred.

9.1 Charging

The battery was connected to the HP6030A supply and charged with a current of 2A

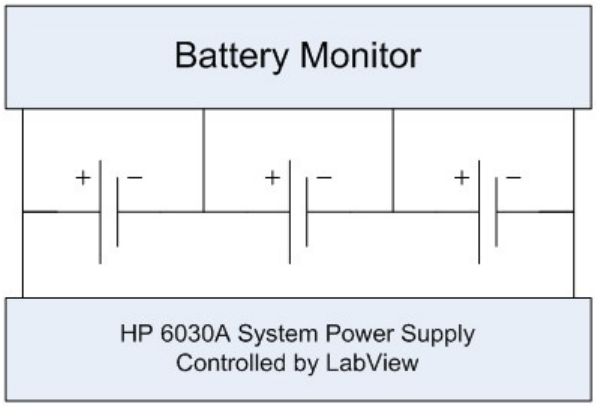

Figure 9.1: Battery charge connection diagram

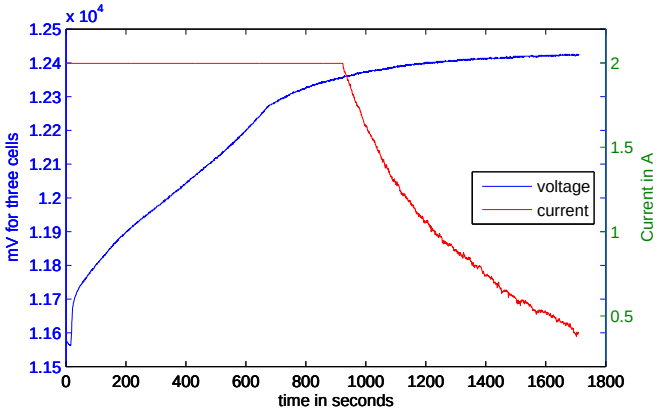

Figure 9.2: Battery charge diagram

One can clearly see the two charge phases. From 0 to 900 seconds the charger is in CC mode, afterwards it enters CV mode. Rise in voltage in CV mode is due to inaccurate power supply regulation

Figure 9.3 manifests that the individual cell voltages of the pack drift away from each

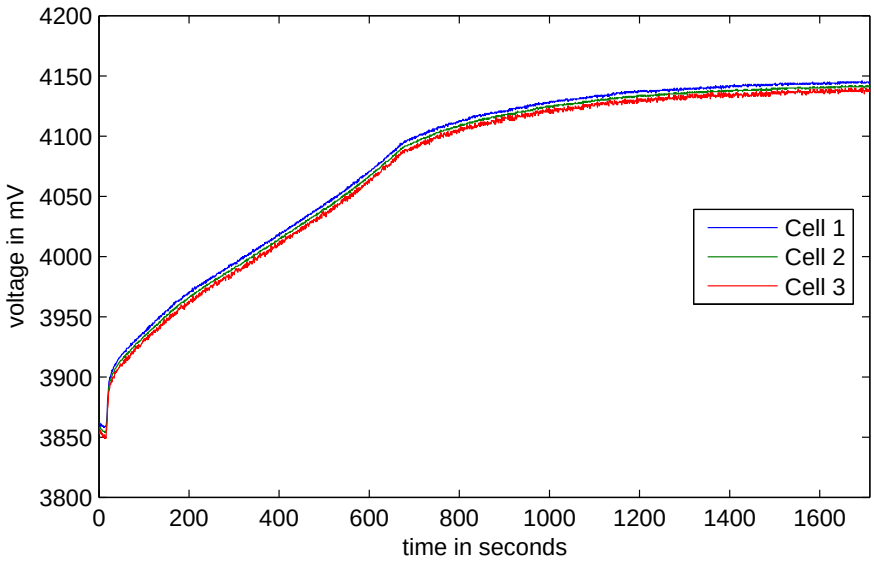

Figure 9.3: Battery charge diagram for individual cells

other while charging. The main reason for this behaviour is the difference in actual capacitance of the cells. The cell with the lowest capacity charges faster and therefore reaches its full charge voltage earlier

9.2 Discharging a single cell

A 10R resistor was connected between terminal 2 and 3 of the battery to discharge a single cell and create an imbalance in the battery pack.

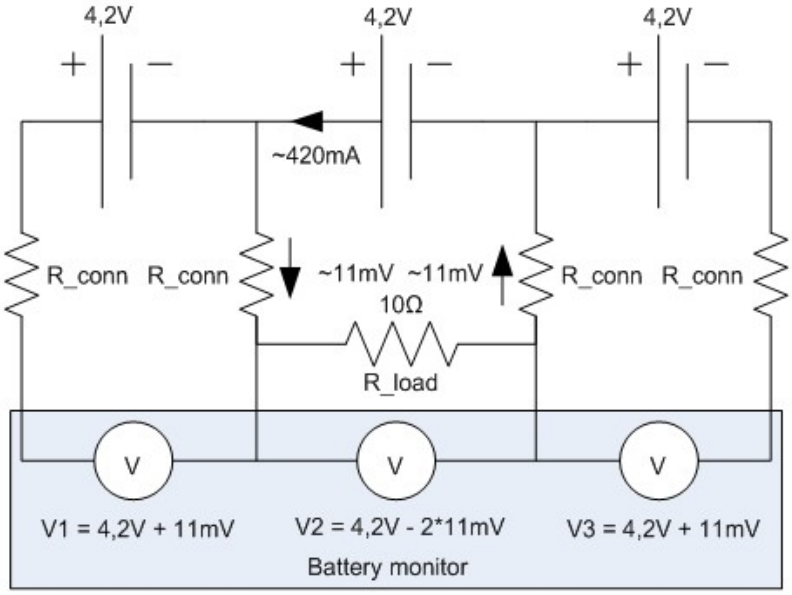

Figure 9.4: Battery discharge connection diagram for individual cells including parasitic resitors

The discharging process can be seen in Figure 9.5

Two effects are worth noticing here:

- The cell that is discharged shows two voltage decreases.
  - First the fast voltage drop due to internal cell resistance and
  - Second the voltage degrading due to sinking SOC.
- It is also worth noticing that the cells adjacent to the battery that is discharged show a minor influence from the discharging process due to the small part of connection cabling they share inside the battery and its resistance (shown in Figure 9.4). The voltage drop across this connection is added to the measured voltage of the adjacent cells (Cell 1 and Cell 3).

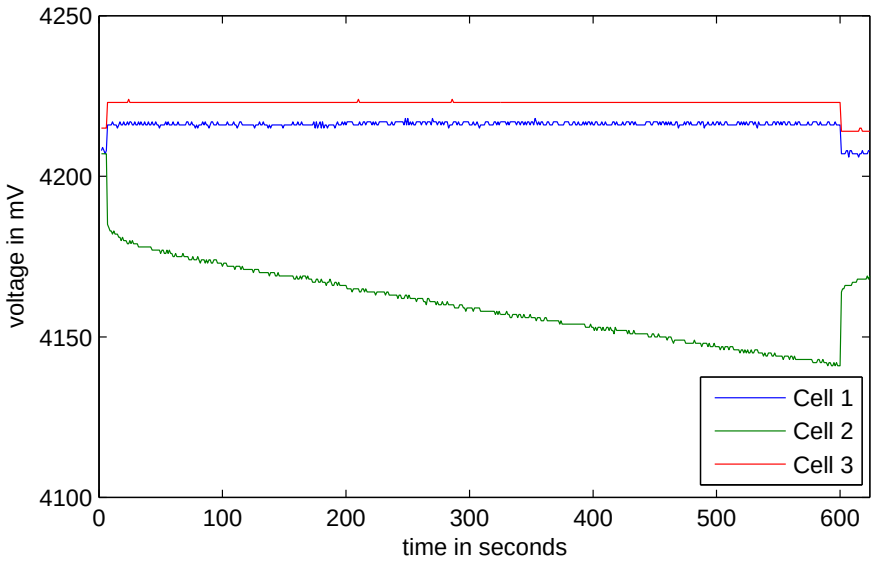

Figure 9.5: Battery disbalanced with single 10R resistor

When choosing a 2,5R resistor to discharge the battery an increase in immediate voltage drop on the discharged cell as well as a higher increase in the voltage of the adjacent cell can be seen.

We can now compare the voltage drops with a 2,5R resistor and the ones with a 10R resistor.

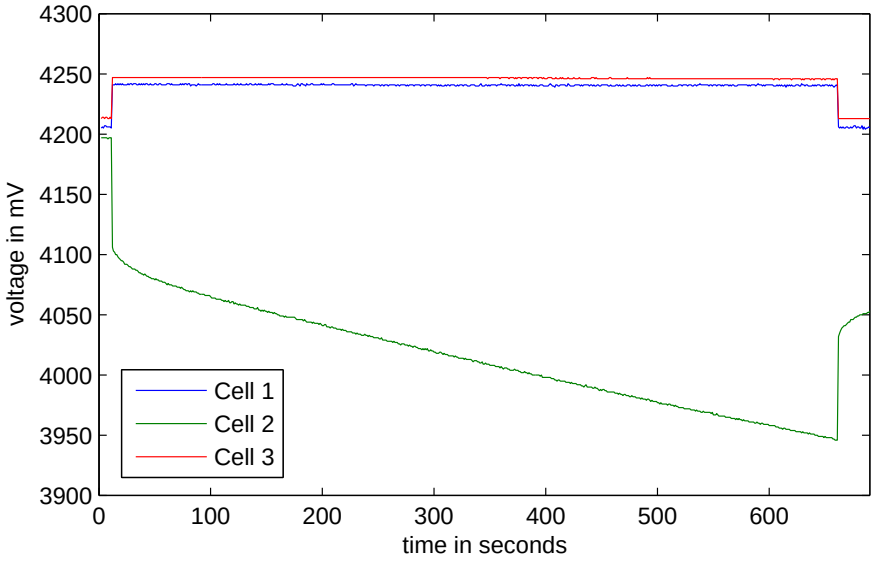

Figure 9.6: Battery disbalanced with single 2R5 resistor

9.3 Discharging a complete battery

The discharge graph shows the three typical parts of a normal battery discharge.

- Stage 1: Fast voltage drop due to internal resistance
- Stage 2: Slow decrease in voltage due to decrease of charge (decrease of material available for REDOX reaction)
- Stage 3: Fast voltage drop at end of discharge when the battery reaches 100% DOD (depth of discharge).

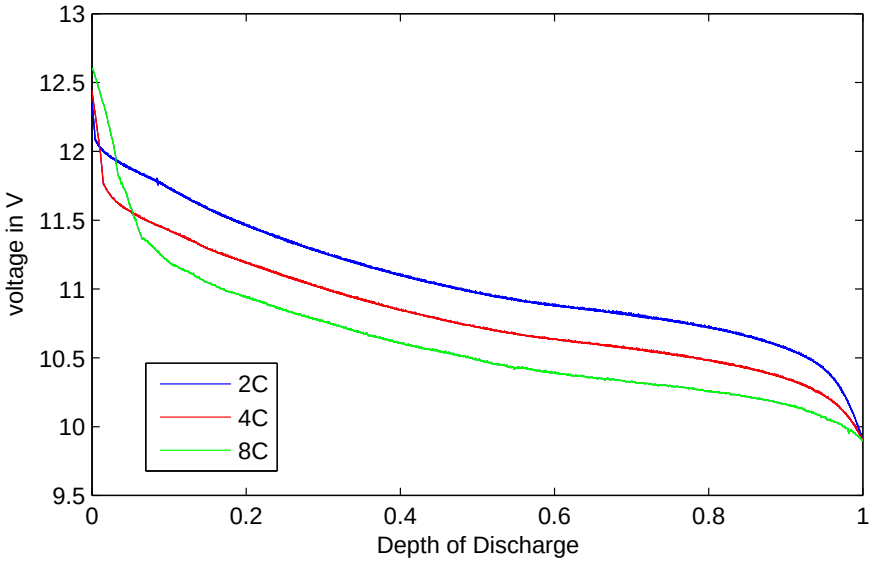

Figure 9.7: Discharge diagram for different discharging rates

9.4 Balancing

After establishing that the test equipment (charger, load and monitor) worked as expected, a test of the balancing process was started.

The test procedure was as follows:

1. Fully charge the battery pack with the system power supply. 2A charge rate, 4,15V per cell charge stop voltage

2. Discharge a single cell or multiple cells via a resistor (as shown in Figure 9.4) 10R for 10 minutes = 70mAh discharge

3. Connect the battery balancer as well as the battery monitor (as shown in Figure 9.8)

4. Balance the battery till the balancer generates the balance done signal

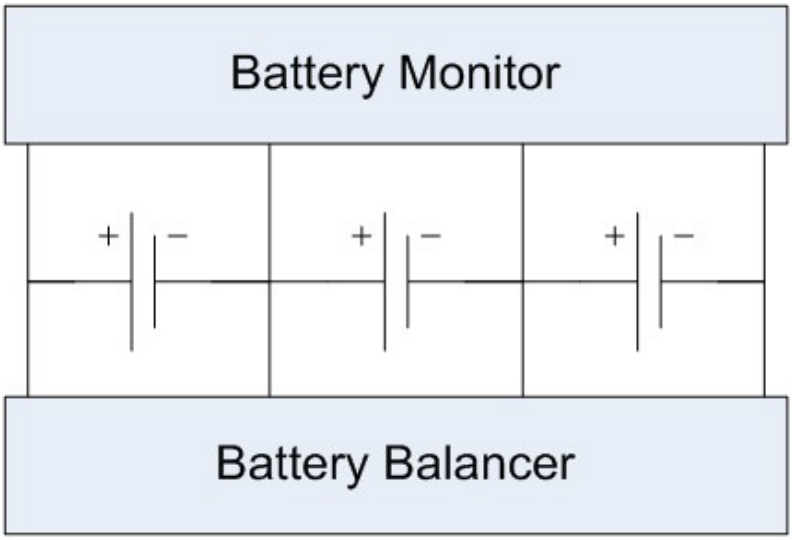

Figure 9.8: Battery balance connection diagram

The active balancing was done with:

- An external power supply directly attached to the transmission gates
- An external power supply powering the DC/DC converter
- The whole battery pack powering the DC/DC converter

Results:

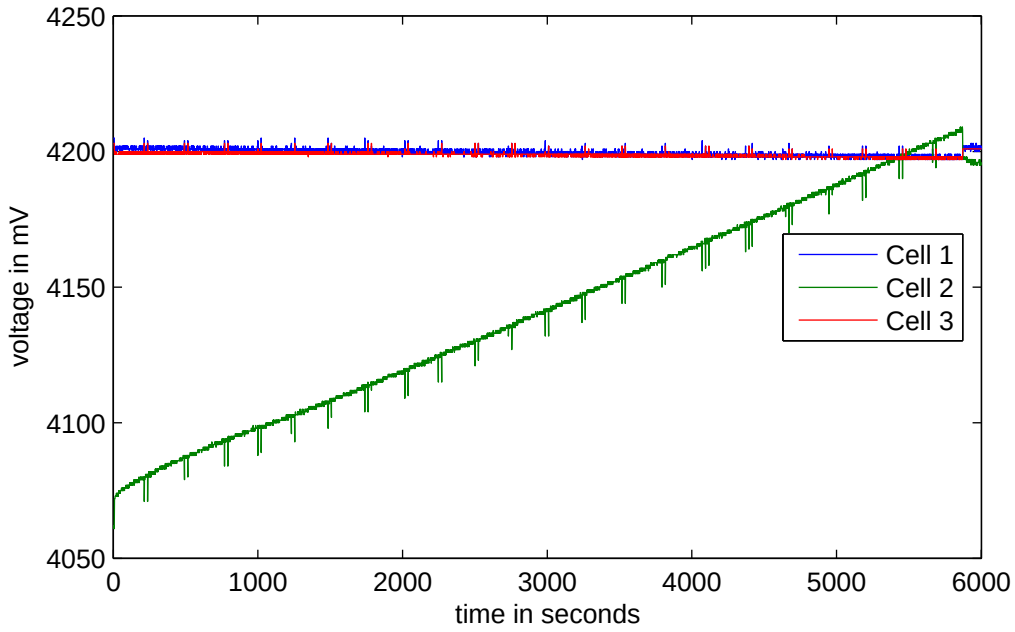

Figure 9.9: Balancing of a single cell after discharging with 2R5

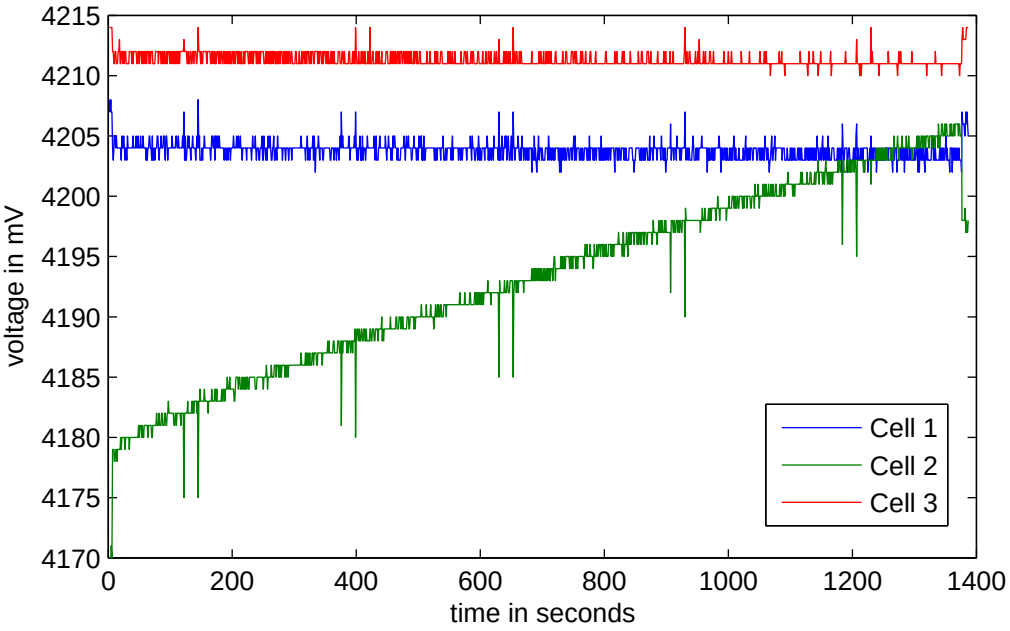

Figure 9.10: Balancing of a single cell after discharging with 10R

It is easy to see that the three individual cell voltages converge versus the average point (which is exactly what is expected). The charge packages delivered to the individual cells by the balancer is displayed in the sudden rise in cell voltage (again due to internal cell resistance).

The balancing algorithm works equally well with a direct external power supply as well as the DC/DC converter powered from either an external supply or the battery pack itself. The noise introduced by the converter can be neglected because the comparison of the individual cell voltage versus mean voltage is only done when the converter is inactive.

The remaining offset in voltage between cells after end of balancing is due to tolerances in the used parts. The two main sources of tolerance are the 0,1% precision resistors (at 4.2 V per cell that means 4.2mV offset) and the comparators with a hysteresis of

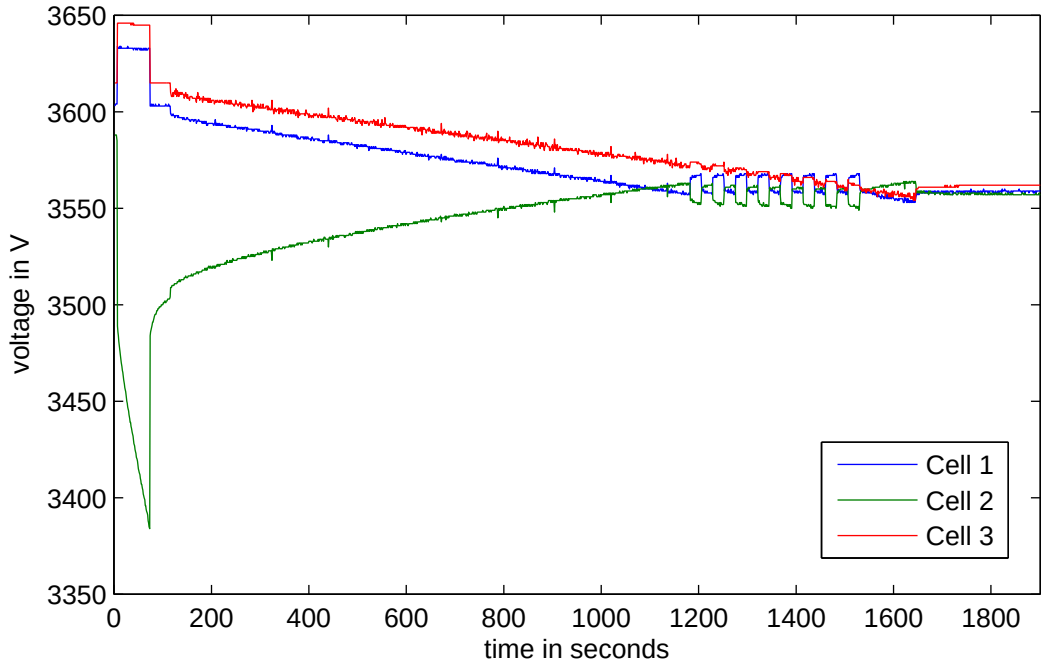

Figure 9.11: Balancing from whole battery to a single cell via DC/DC converter

3mV.

The influence (noise ripple and voltage degrading) on the cells not being balanced is again mainly due to the part of connection cabling they share with the cells being balanced.

9.5 Influence of capacity for misbalancing

In order to find out if the main reason for misbalance is the difference in capacity between cells in a pack the following measurements were done.

1. Bring the battery to a defined SOC. In our case that was 3.5V per cell
2. Balance the battery pack
3. Charge the battery pack to 100% SOC
4. Measure the misbalance
5. Discharge the battery pack to the defined SOC in point 1
6. Measure the misbalance if there is any
7. Balance the battery pack and check how much charge was needed to balance the battery

In a second test we discharged the battery to 10% SOC, measured the misbalance, charged it a gain to the defined SOC and measured the misbalance again.

These measurements were done with the same setup as described in Figure 9.8.

9.6 Balancing while charging/discharging

The measurements were done as follows:

1. Discharge a single cell or multiple cells via a resistor (as shown in Figure 9.4) 10R for 10 minutes = 70mAh discharge

2. Full charge of the battery (to get a reference charge curve with disbalanced cells) 1A charge current 4,15V per cell end voltage

3. Full discharge of the battery down to 10% SOC, (to get a reference for the next measurement)
   4A discharge current, 3V per cell end voltage

4. Full charge of the battery with the same charge data as above while balancing 100mA balancing current

and

1. Discharge a single cell or multiple cells via a resistor (as shown in Figure 9.4) 10R for 10 minutes = 70mAh discharge

2. Full charge of the battery
   1A charge current, 4,15V per cell end voltage

3. Full discharge of the battery down to 10% SOC with the balancer enabled 4A discharge current, 3V per cell end voltage, 100mA balancing current

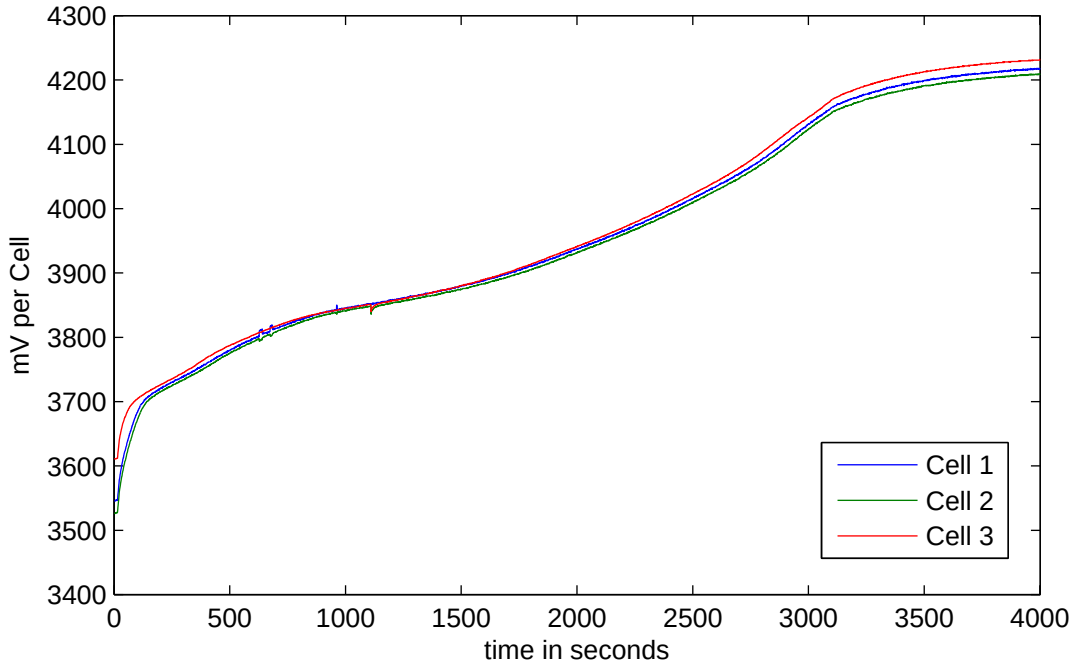

Figure 9.12: Charge cycle with 2A charging current without balancing

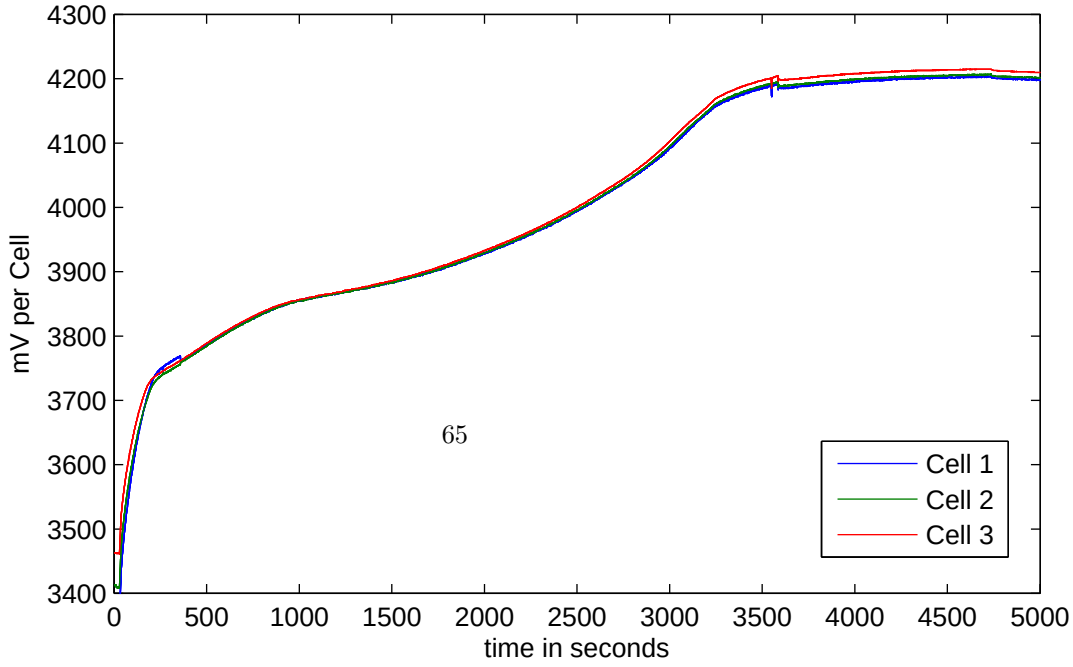

Figure 9.13: Charge cycle with 2A charging current with balancing

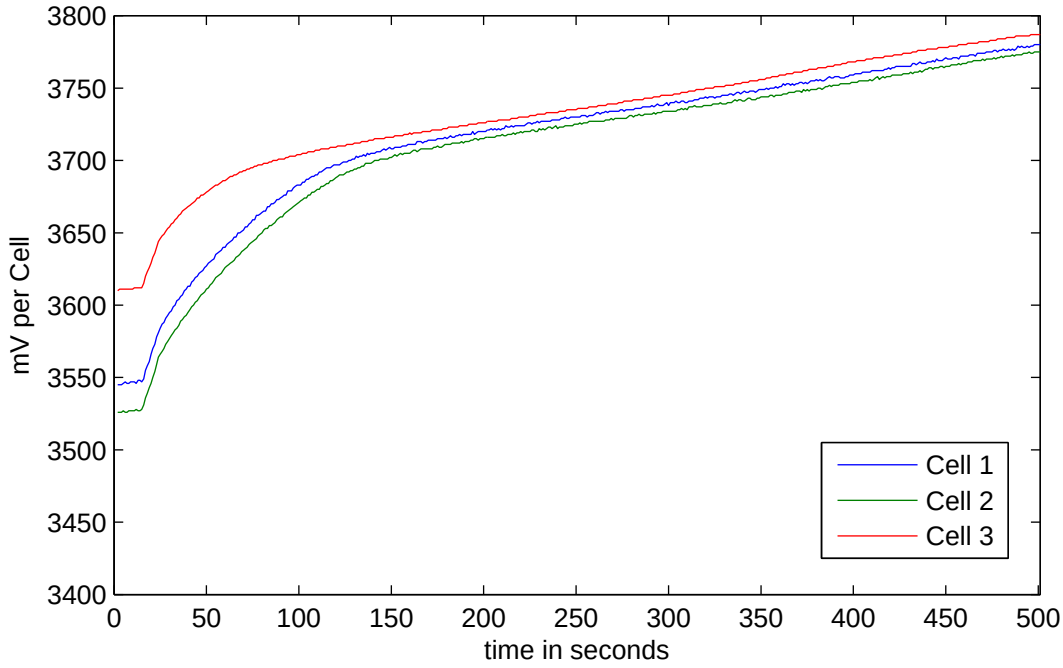

Figure 9.14: First 500 seconds of Figure 9.12

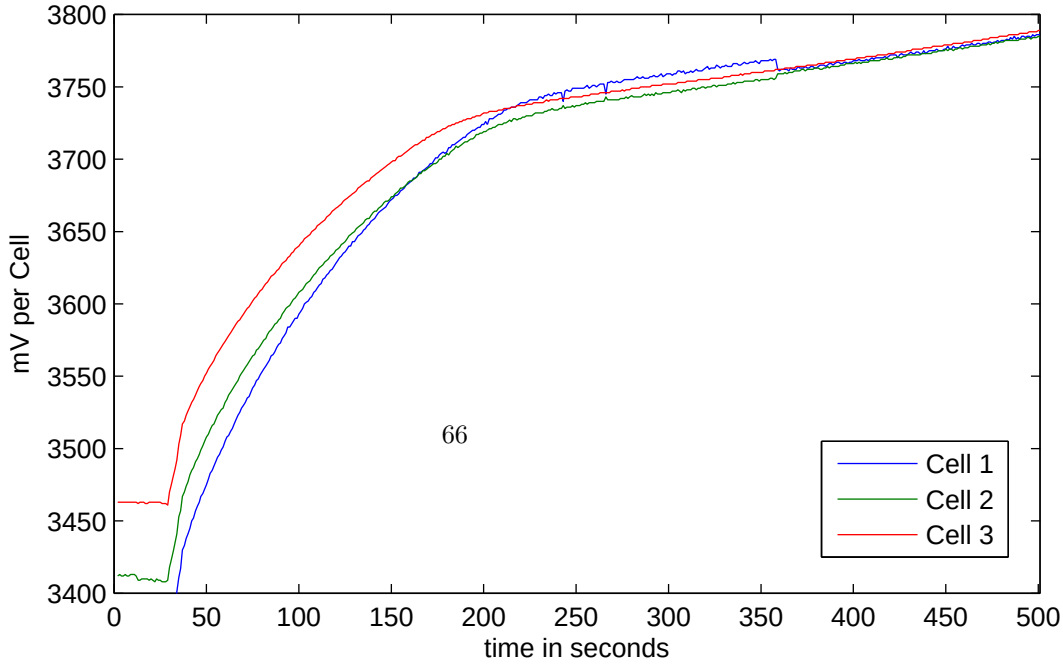

Figure 9.15: First 500 seconds of Figure 9.13

10 Conclusion

From the measurements done we can conclude that the approach we took (analog comparison of voltages combined with active charging of the weakest cells) is a valid working concept to stop cell voltage drift and therefore make the maximum capacity of a battery pack accessible. The concept works equally well under all three possible battery load conditions (charging, idle and discharging). The disadvantage of a higher cost of external parts as well as cabling is compensated by lower losses in the batter managing process (reuse of energy versus waste of energy in heat) and the possibility to build a standalone balancing solution without the need of a microcontroller and custom firmware. With the implementation of this concept into an IC it makes a winning alternative to classic battery balancing concepts.

Bibliography

[1] Lithium Batteries
http://en.wikipedia.org/wiki/Lithium-ion_battery

[2] Charge a battery in just six minutes by Duncan Graham-Rowe
http://www.newscientist.com/article/dn7081

[3] Lithium air batteries
http://www.almaden.ibm.com/institute/resources/2009/presentations/StevenVisco-AlmadenInstitute2009.pdf

[4] How to rebuild a Li-Ion battery pack
http://www.electronics-lab.com/articles/Li_Ion_reconstruct/

[5] SMBus Specifications
http://smbus.org/specs/

[6] State of Health (SOH) Determination
http://www.mpoweruk.com/soh.htm

[7] Lithium Battery Failures
http://www.mpoweruk.com/lithium_failures.htm

[8] Thermal Runaway by S Tobsihma, Gunma University Kiryu Japan Encyclopedia of electrochemical power sources 2009 Volume 5

[9] Energy Density Comparison
http://www.nexergy.com/battery-density.htm

[10] LCD-library
http://www.jump.to/fleury

[11] Flyback Converter
http://www.pes.ee.ethz.ch/fileadmin/user_upload/pes/education/fple/IE5_Flyback_Script.pdf

[12] Design for EMC and LVD
http://www.ami.ac.uk/courses/ami4966_emclvd/u02/

[13] Kaschke catalogue
http://www.kaschke.de/pdf/Katalog2010.pdf

[14] Wuerth electronic catalog
http://katalog.we-online.de/kataloge/eisos/media/pdf/749196111.pdf

[15] Wuerth WE-Flex designer
http://www.we-online.com/web/en/index.php/download/media/import/emc/download_verstecke_seiten/The_WE-FLEX_Designer_2.zip

List of Figures

11 Appendix

11.1 Balancer Schematic and Layout

11.2 Battery Monitor Schematic and Layout

11.3 AS8510 Demo Board Schematic after rewiring

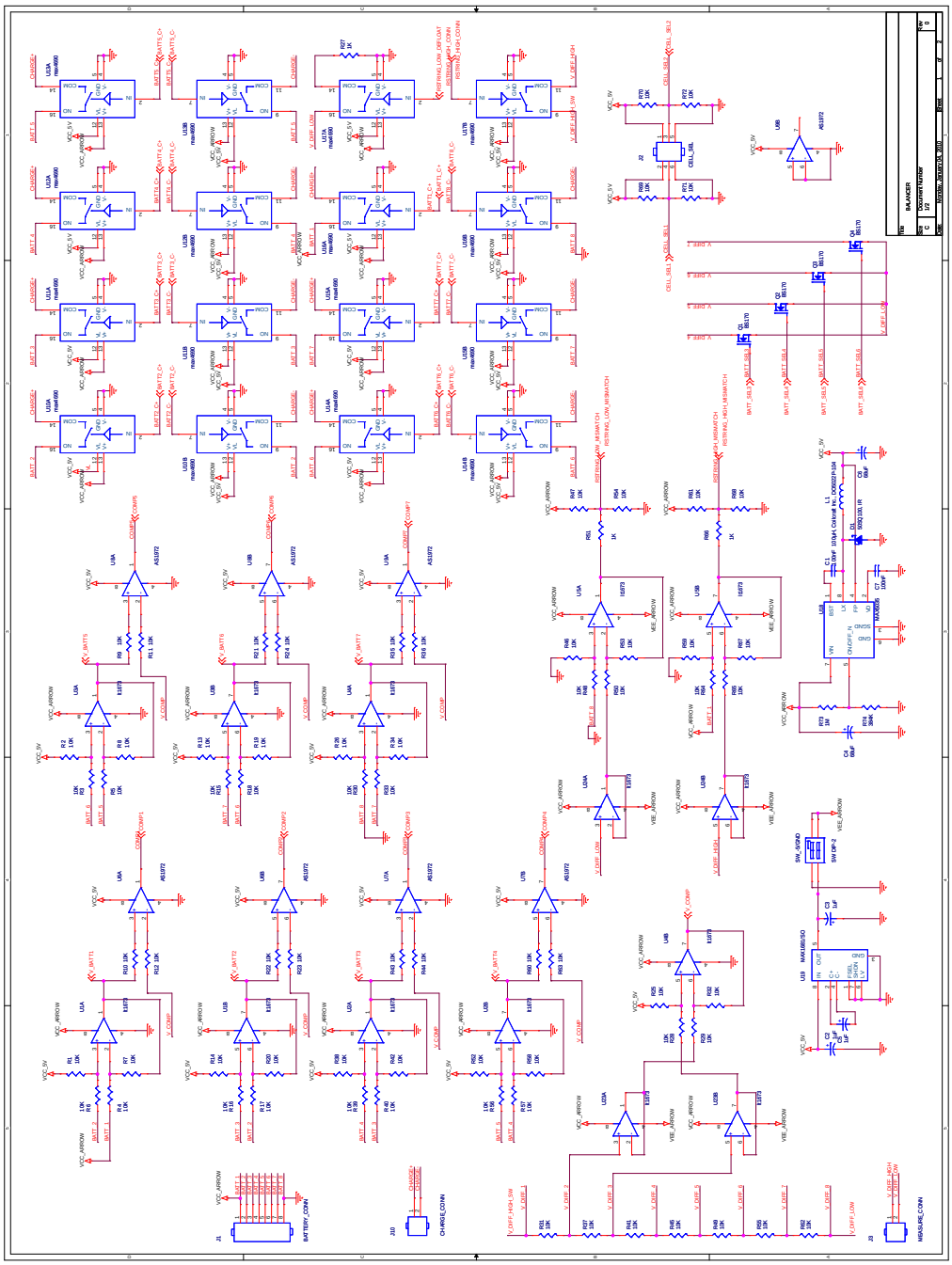

Figure 11.1: Battery Balancer Schematic Page 1

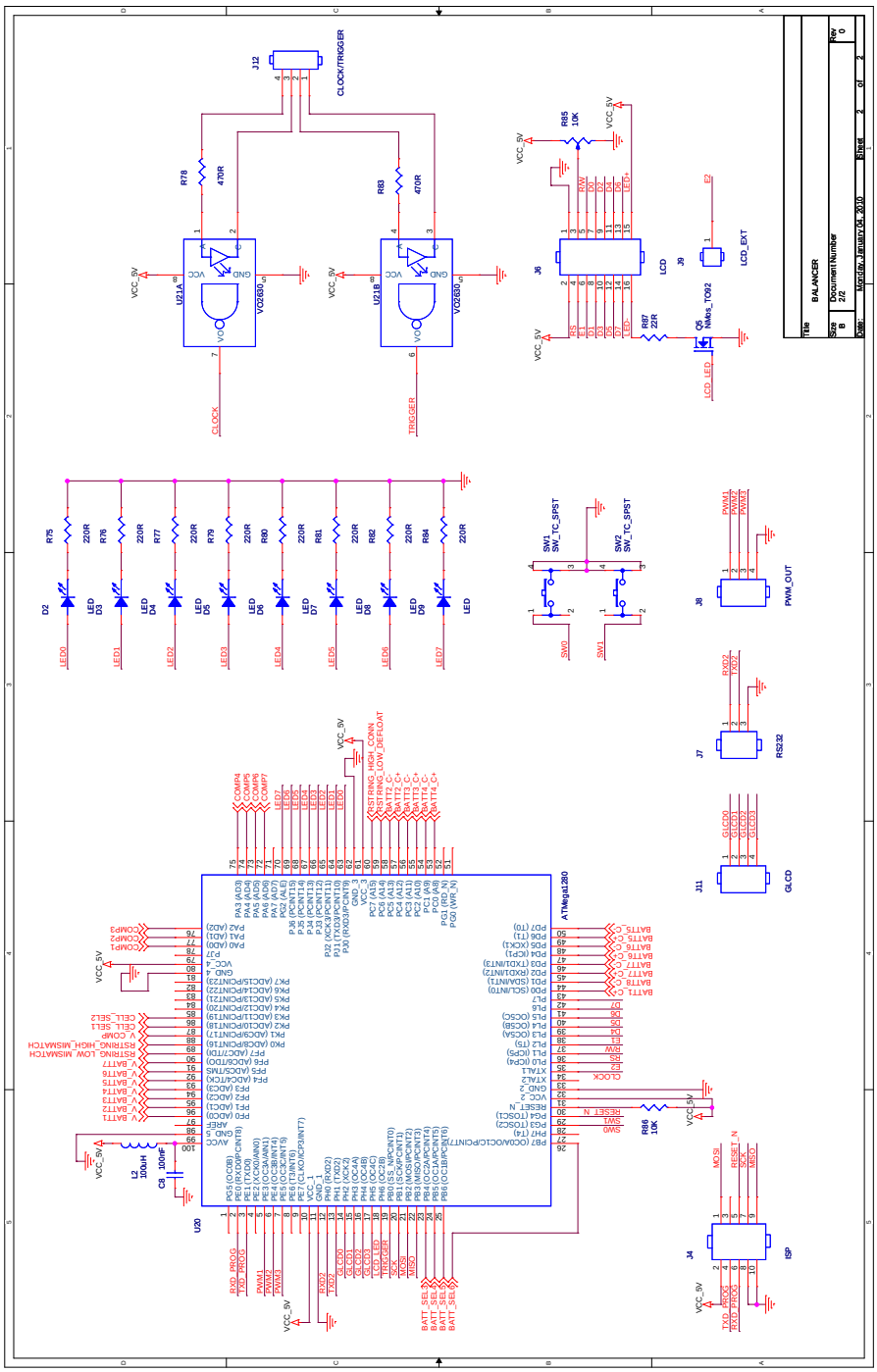

Figure 11.2: Battery Balancer Schematic Page 2

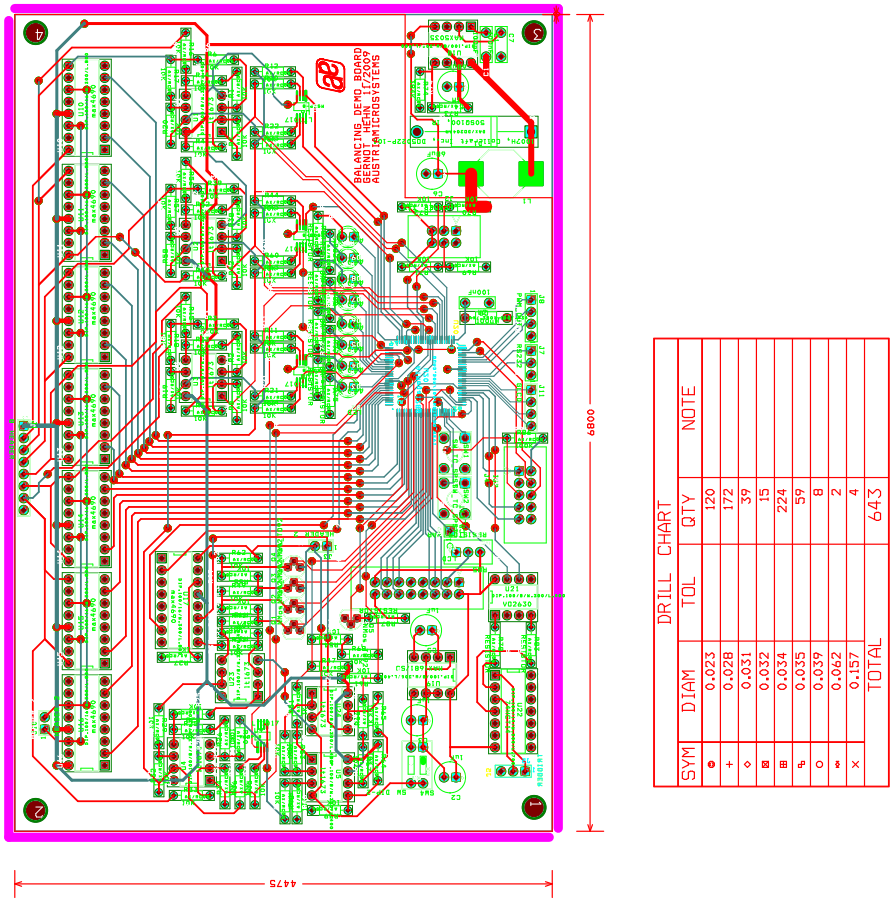

Figure 11.3: Battery Balancer Layout

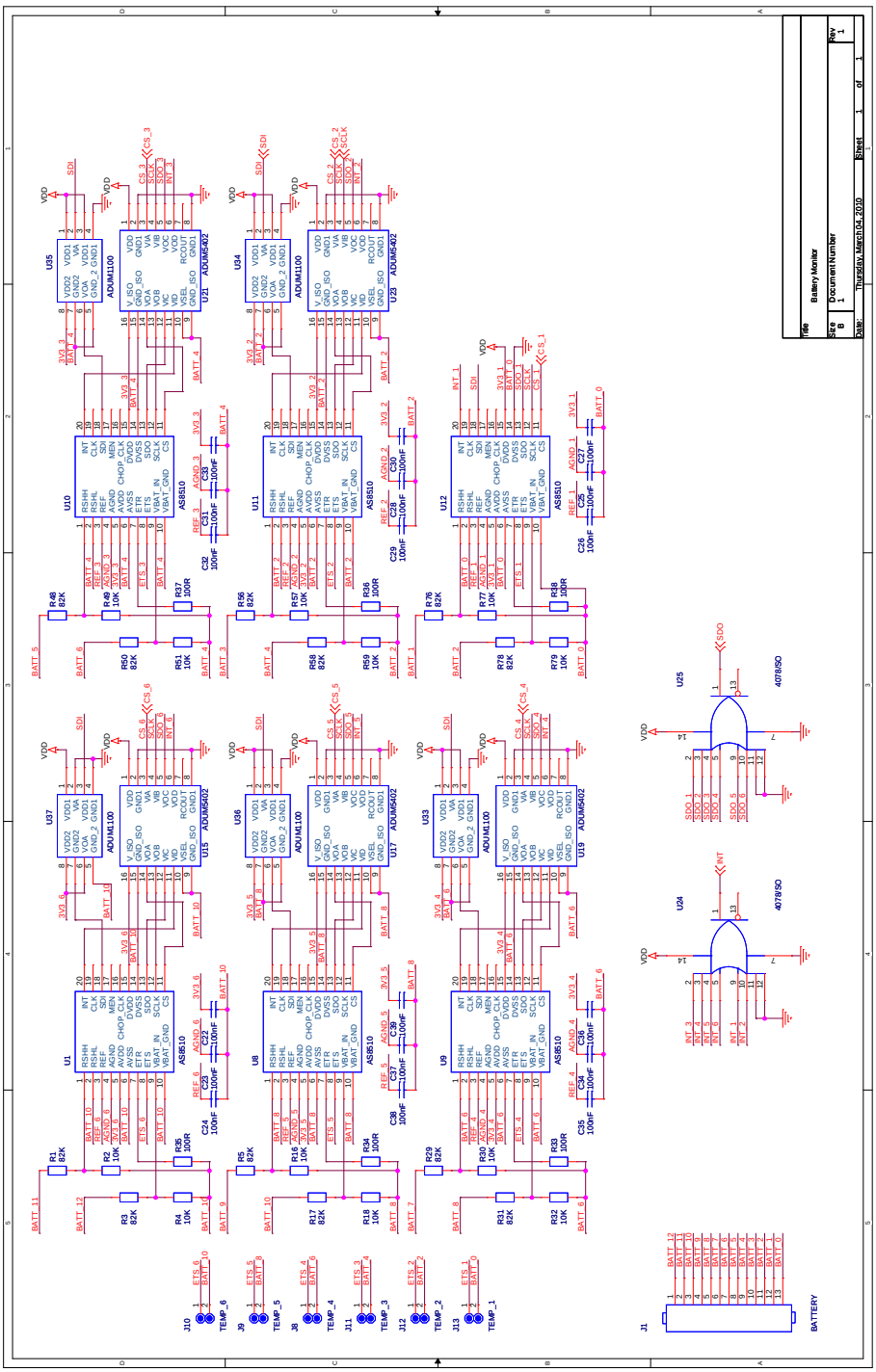

Figure 11.4: Battery Monitor Schematic Page 1

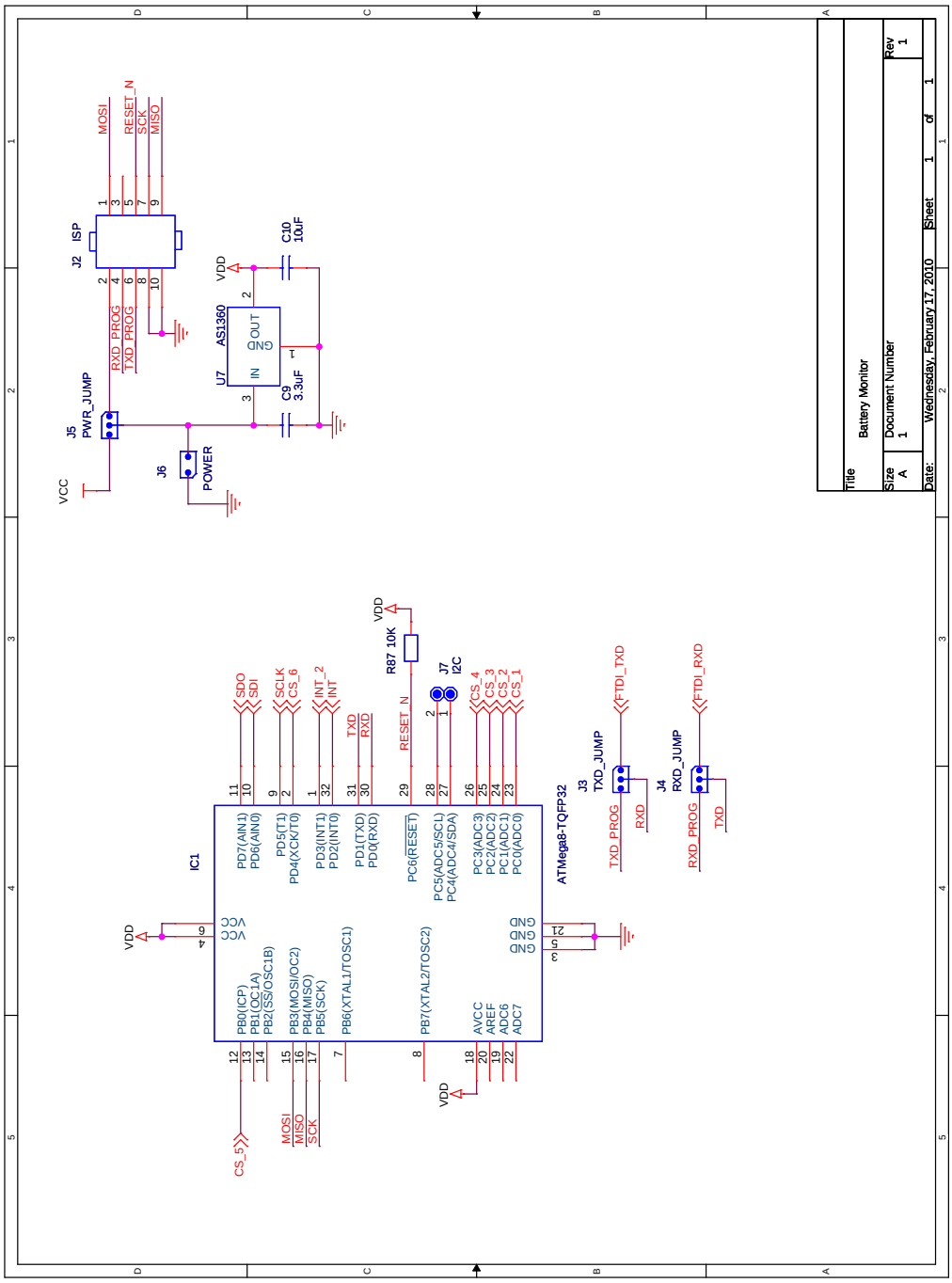

Figure 11.5: Battery Monitor Schematic Page 2

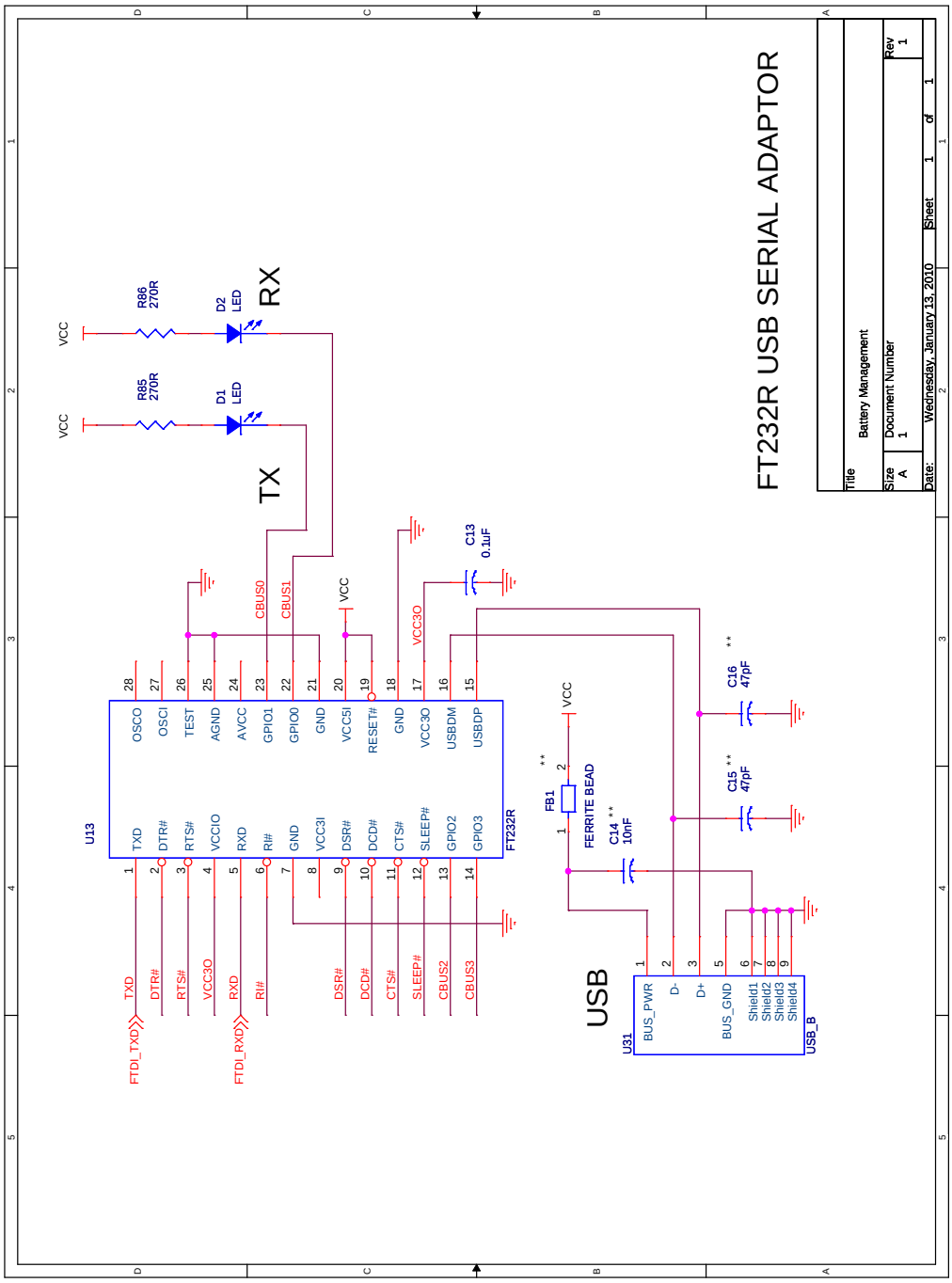

Figure 11.6: Battery Monitor Schematic Page 3

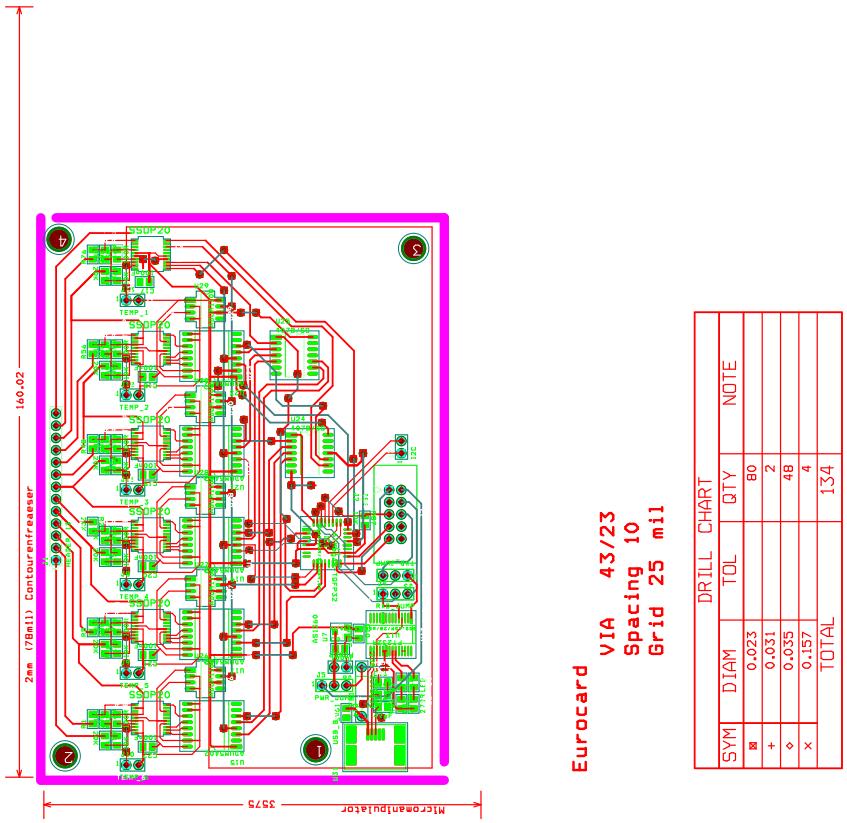

Figure 11.7: Battery Monitor Layout

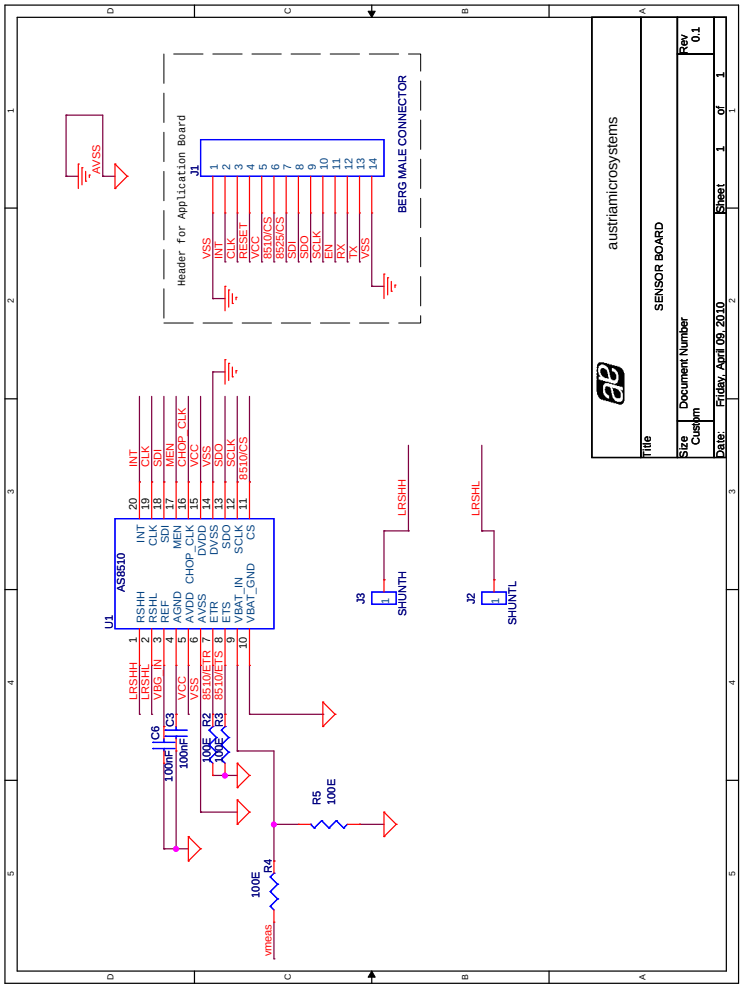

Figure 11.8: AS8510 Demo Board after rewiring Schematic Page 1

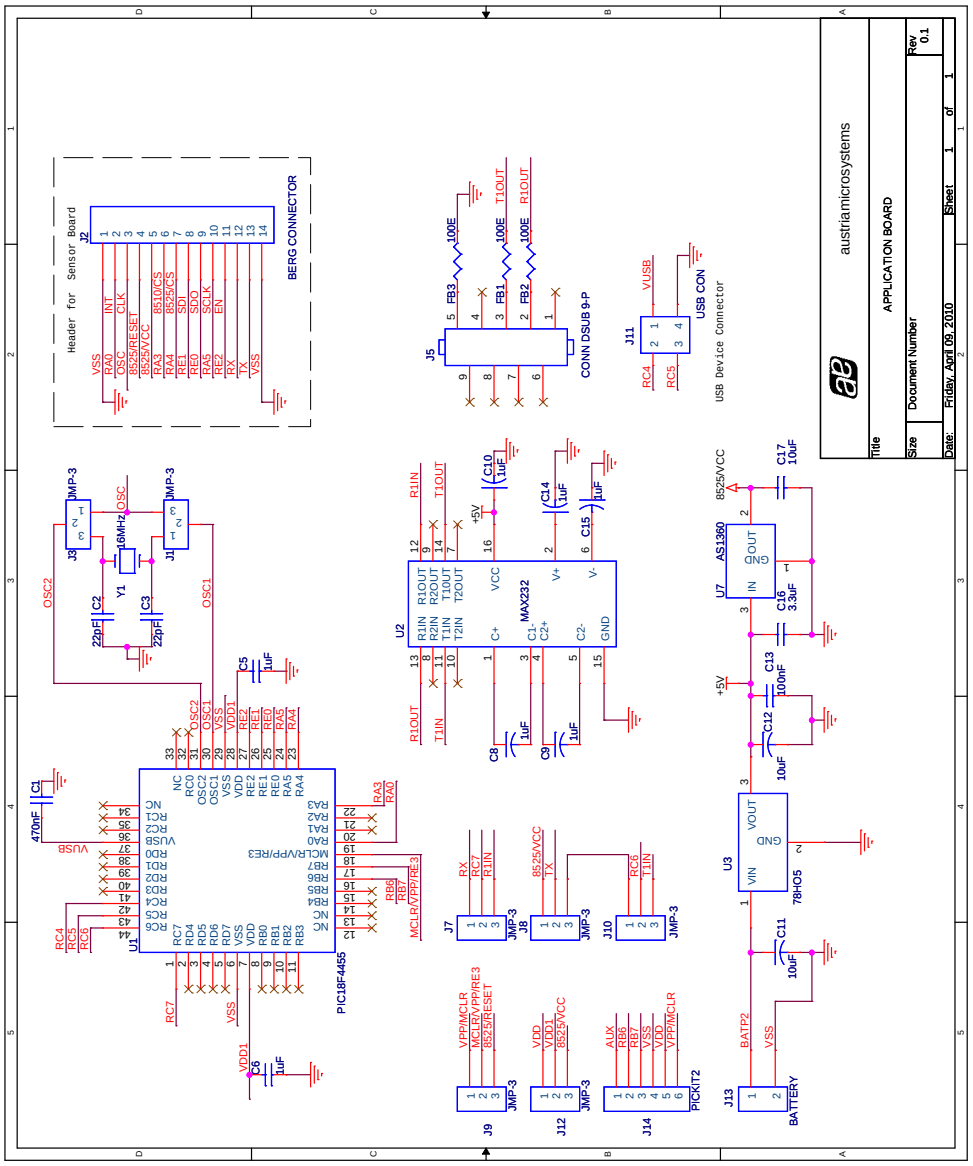

Figure 11.9: AS8510 Demo Board after rewiring Schematic Page 2